27 copies

NASA CR-66319

C7-478/201 Copy No. 25

FINAL REPORT FOR PHOTOCONDUCTOR CONFIGURATION STUDY

February 28, 1967

North American Aviation, Inc. Autonetics Division
3370 East Miraloma Avenue, Anaheim, California 92803

Contract No. NAS 1-5314

FOREWORD

The final report for the Photoconductor Configuration Study was prepared under Contract NAS 1-5314.

ABSTRACT

The objective of the Photoconductor Configuration Study was to evaluate several volume effect, cadmium sulfide, position sensitive photodetectors for space star-tracking applications. A position sensitive detector indicates both the presence of a star image and the position of the image on the photodetector.

Five photodetectors were fabricated and evaluated in both single-axis and two-axis detection configurations. A description of volume effect, cadmium sulfide photoconductors, the theory of each detection technique, fabrication processes, test procedures, and test results are presented. The test results are discussed and evaluated. Recommendations for further work are also presented.

CONTENTS

CONTENTS (Continued)

ILLUSTRATIONS

ILLUSTRATIONS (Continued)

TABLES

I. INTRODUCTION

The objective of the study program was to evaluate and determine the inherent error in several configurations of position sensitive volume effect detectors. Applications of a detector of this nature lie mainly in space star-tracking applications, i.e., the detection of a star against an essentially dark background.

A position sensitive detector detects both the presence of a star image and the position of the image on the detector. The output of the detector is required to contain the position information with equal accuracy over the entire active area. The approach which was evaluated in this study is the use of volume effect, cadmium sulfide photoconductive material. In the volume effect mode of operation, a large area device can be fabricated without a loss in sensitivity.

In the course of this investigation, five devices were evaluated in three position sensitive detector configurations. All five were tested in both single axis and two axis position sensitive modes of operation.

This report contains a description of volume effect photoconductors, the theory of each detection technique, detector fabrication details, and test procedures and results.

The knowledge gained in the study program is summarized in the Conclusions section. The test results are discussed and evaluated, and recommendations are made for further work toward making the position sensitive photodetector a practical device.

II. VOLUME EFFECT PHOTOCONDUCTORS

In general, photoconductivity or the modulation of the bulk conductivity of a material with incident photons of sufficient energy, is a well understood process. For a review of this subject see Ref. 1, 2, and 3. When photoconductivity is applied to practical detectors, there are many factors which cannot be completely analyzed and must be treated empirically.

The surface effect photodetector is the most common type now in use. In surface effect detectors the photoconductive film is deposited directly on the glass substrate. Metallic electrodes are deposited on the surface of the photoconductive film. A bias voltage is applied between these electrodes, causing the photocurrent to flow in the plane of the film. For a given voltage, the photocurrent is inversely proportional to the square of the inter-electrode spacing. To get a suitable star signal the electrode spacing must be approximately the same size as the star image (typically 1 mil). This factor eliminates the possibility of using large active area surface effect detectors. It is possible to fabricate an array of surface effect devices, but the percentage of inactive regions becomes high due to the presence of electrodes on the surface.

Volume effect detectors differ from surface effect detectors in that the photoconductive film is deposited on a transparent conductive film on the glass substrate. A metallic electrode is deposited on the surface of the photoconductor and the bias voltage is applied between it and the transparent conductor. A star image is incident on the photoconductive film through the glass substrate and the transparent conductor. The photocurrent is normal to the plane of the film and the electrode spacing (i.e., the film thickness) is constant regardless of the size of the active area of the detector. It is this property that makes the volume effect detector the most attractive for star tracking applications in space.

Cadmium sulfide (CdS) was the photoconductive material studied in this program. Tin oxide was utilized as the transparent conductive material.

The key to fabrication of a practical volume effect device is to be able to deposit a thin film of photoconductive material on the transparent electrode without contamination of one material by the other. The photoconductor is then sensitized by standard doping techniques. A metallic electrode is deposited on the photoconductive film to complete the "sandwich". Once a complete understanding of all of the very complex material interactions

is known, an ideal volume effect detector can be fabricated. The volume effect detector will make possible many future applications which would not have been practical using conventional surface effect detectors.

Descriptions of the volume effect photoconductor material usage, fabrication and detection techniques are presented in the following sections of this report.

III. POSITION SENSITIVE DETECTOR TECHNIQUES

A position sensitive detector not only indicates the presence of a star image but also presents a readout of the position of the image. Position sensitivity is required in an application where the star image can be at any position within the telescope field-of-view and the position of the star image must be determined without any motion of the telescope. A large area detector which covers the entire field-of-view must be used for this application. The requirement of the large area device is best satisfied by using volume effect photoconductors as described in section II.

Position information can be extracted from volume effect detectors by using the following technique: An electric field pattern is generated in the tin oxide film under the CdS so that the field is unique in any position. If a star image is incident on the CdS film, the CdS at that point is highly conductive as compared to the rest of the active area which sees a black background. The metal electrode on top of the CdS film takes on the potential of the tin oxide at the point of star incidence. Thus, the potential of the metal electrode is a direct measurement of the star position.

The two major design considerations of position sensitive, volume effect detectors are: (1) the generation of an electric field which is unique at any point, and (2) the coupling of this field to the output electrode without perturbations due to nonuniformity in the tin oxide or CdS films, contact resistance variations, and other factors which would distort the position information.

The various techniques which have been used to generate the required electric field are described in this section. Later sections will discuss the practical problems which introduce errors into the operation of the device.

A. SINGLE-AXIS ELECTRIC FIELD DETECTOR

The simplest position sensitive detector is a single-axis dc detector. A detector of this type will provide a position readout in one dimension only; however, the importance of this detection scheme should not be overlooked. At the present time, the single-axis device is the most accurate due to its simplicity. A two-axis system can be fabricated using a beam splitter and two detectors with orthogonal sensitive axes.

A single-axis dc detector is shown in Fig. 1. A bias voltage is applied between the two outer metal electrodes, resulting in equipotential lines between the electrodes as shown by the dash lines in the figure. A star image incident on the detector causes the metal electrode on the active area to take on the potential of the equipotential line at that point. This potential gives the star position in the sensitive axis of the detector. An analysis of the electric field pattern in the tin oxide is quite straightforward for this configuration and is developed below.

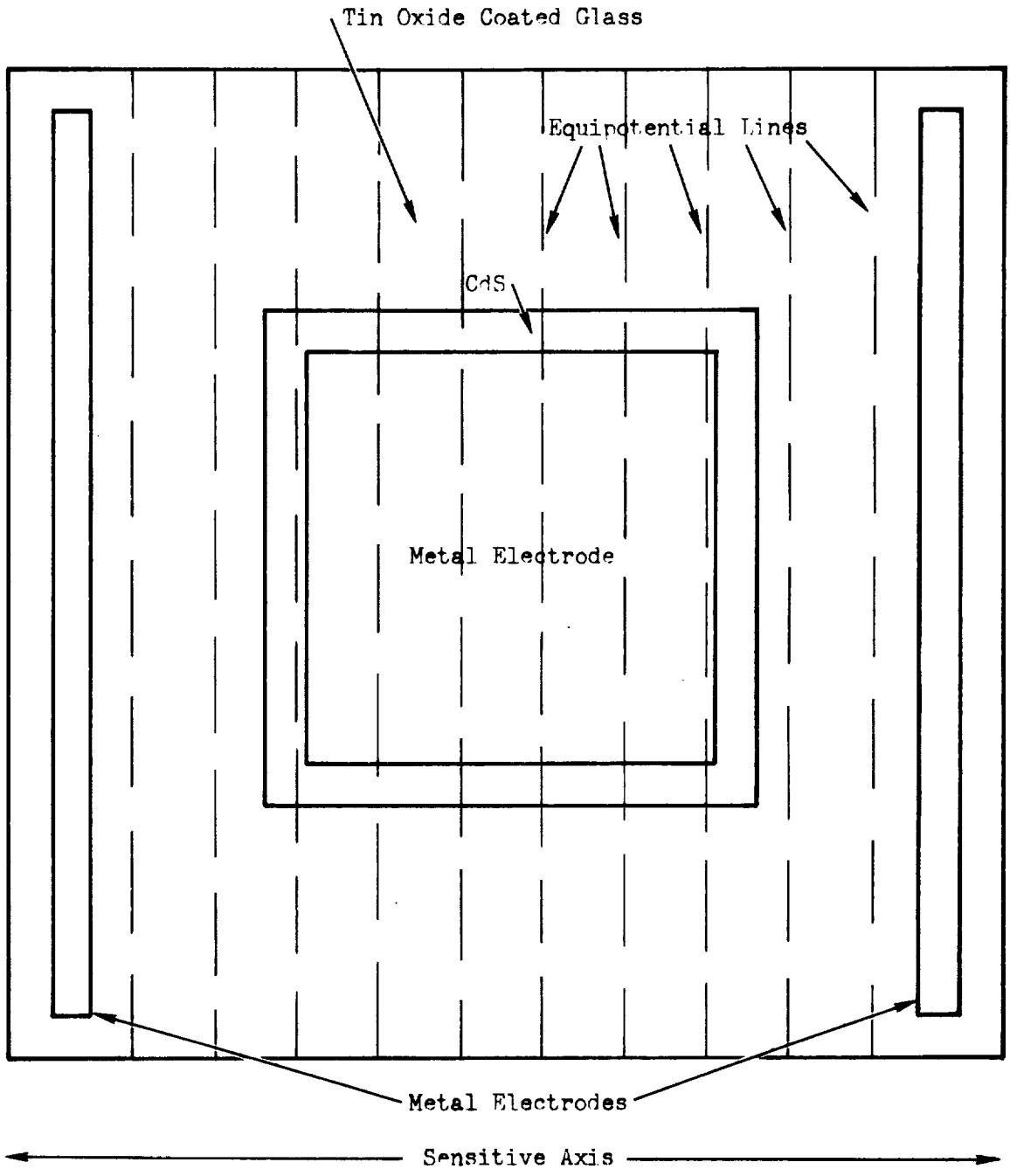

Fig. 1. Single-Axis DC Detector

The photodetector shown in Fig. 2 will now be considered. There are two paths for current to flow in this device, one path through the tin oxide film to ground, and one path through the cadmium sulfide and load resistor to ground. The purpose of the analysis is to determine the current flow and potential distribution characteristics of this device. It is assumed that current and potential are functions of x only. The following equations are presented:

$$\frac{dI}{dx} = -G(x) \left[V(x) - V_{out}\right] \tag{1}$$

$$\frac{dV}{dx} = -R \left[I(x)\right] \tag{2}$$

$$V_{out} = I_T R_L \tag{3}$$

where

$I(x)$ = current flow within the tin oxide layer, which usually decreases monotonically as the current is shunted through the cadmium sulfide

$V(x)$ = potential variation along the tin oxide layer

$G(x)$ = conductance per unit length along the x direction of the cadmium sulfide. This is given by $\frac{W \sigma_2(x)}{t}$ where the conductivity of the CdS, $\sigma_2(x)$, is a function of x only

R = resistance per unit length of the tin oxide $(\sigma_1 \, Wd)^{-1}$

σ_1, σ_2 = conductivities of the tin oxide and CdS, respectively

R_L = output load resistance

I_T = total current flowing through R_L

The output current, I_T, can be obtained by taking the negative integral of equation 1. It is negative since a decrease in $I(x)$ must increase I_T.

$$I_T = -\int_0^L \left(\frac{dI}{dx}\right) dx = \int_0^L G(x) \, V(x) \, dx - I_T R_L \int_0^L G(x) \, dx \tag{4}$$

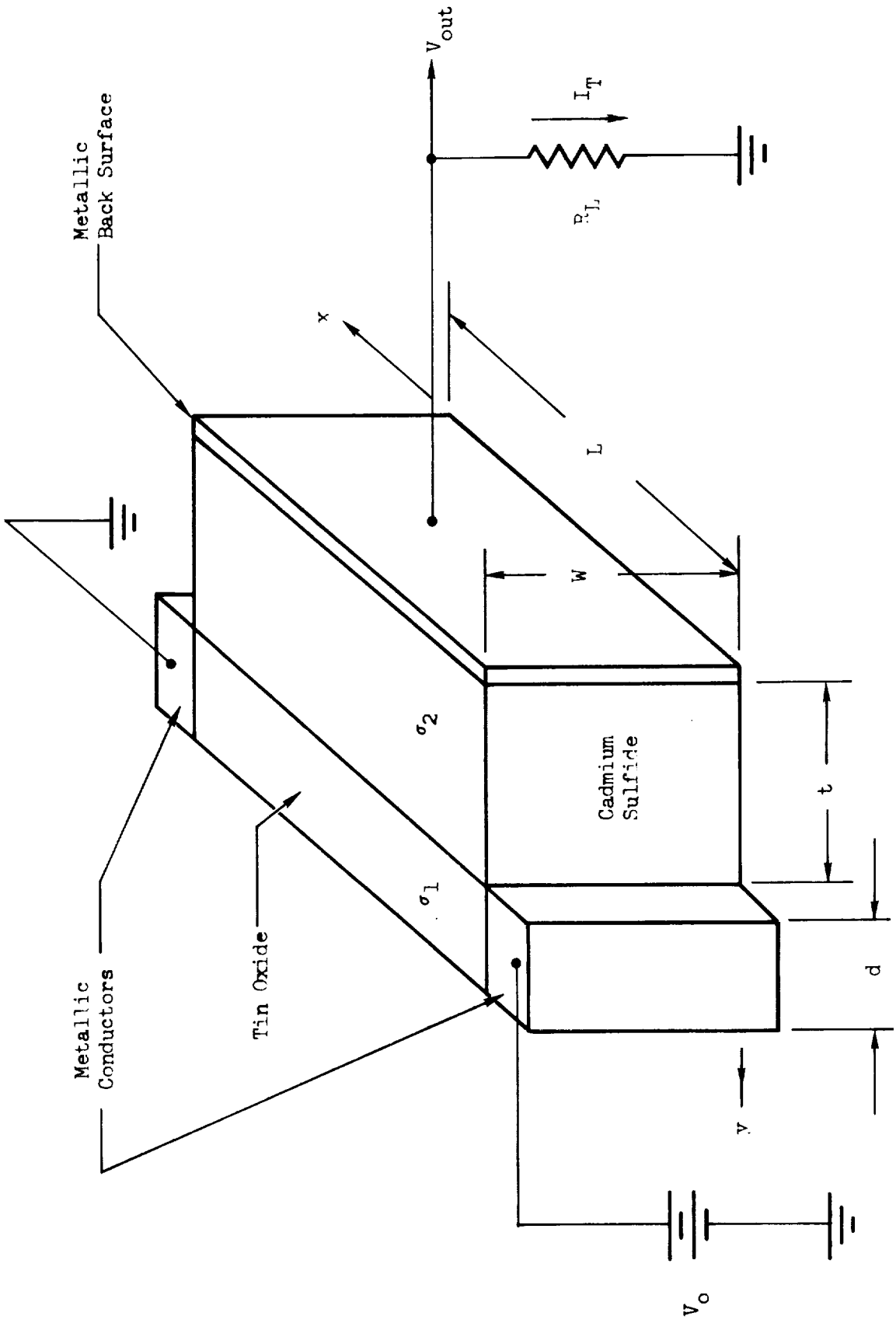

Fig. 2. Schematic of Single-Axis Volume Effect Photodetector

Consider that

$$\int_0^L G(x)\, dx = \frac{1}{R_s} \tag{5}$$

where R_s is the resistance of the CdS. Hence,

$$I_T = \frac{R_s}{R_s + R_L} \int_0^L G(x)\, V(x)\, dx \tag{6}$$

The corresponding output voltage is

$$V_{out} = \frac{R_s\, R_L}{R_s + R_L} \int_0^L G(x)\, V(x)\, dx \tag{7}$$

The potential variation, V(x), is derived from a solution of the second-order differential equation resulting from the combination of Eq. (1) and (2):

$$\frac{d}{dx}\left[\frac{1}{R}\frac{dV}{dx}\right] - G(x)\, V(x) = -G(x)\, V_{out} \tag{8}$$

with the solution being subject to the boundary conditions

$$\begin{aligned} &\text{(i)}\ V(0) = V_o \\ &\text{(ii)}\ V(1) = 0 \end{aligned} \tag{9}$$

The conductivities, σ_1 and σ_2, (see Fig. 2) are assumed to be uniform throughout the respective materials. Using this assumption, eliminating the current I(x) from Eq. (1), (2), and (3) leads to

$$\frac{d^2V}{dx^2} - \beta^2 V = -\beta^2 V_{out} \tag{10}$$

where

$$\beta = \sqrt{RG}\,\sqrt{\frac{\sigma_1}{\sigma_2}}\,\frac{1}{td} \tag{11}$$

The solution for V(x) is of the form $V(x) = A \cosh \beta x + B \sinh \beta x$ which, upon application of the boundary conditions [Eq. (9)], reduces to

$$V(x) = V_o \frac{\sinh \beta(L - x)}{\sin \beta L} + V_{out}\left\{1 - \frac{\cosh \beta\left(\frac{L}{2} - x\right)}{\cosh \beta \frac{L}{2}}\right\}. \tag{12}$$

The corresponding output current and potential can be obtained by substituting this last expression into Eq. (5) and (6), respectively.

It is interesting to note that if the CdS material is assumed to be nonconducting,

$$\beta = \sqrt{\frac{\sigma_1}{\sigma_2} \frac{1}{td}} \rightarrow 0 \tag{13}$$

Then

$$V(x) \rightarrow V_o \frac{\beta(L-x)}{\beta L} + V_{out} (1 - 1) \tag{14}$$

or

$$\lim_{\beta \rightarrow 0} V(x) = V_o \left(1 - \frac{x}{L}\right). \tag{15}$$

At this point, it is of interest to calculate β by using actual values to determine the deviation from linearity which arises from conduction through the CdS material. The dark current in a detector which is 100 mil on a side is typically 5×10^{-10} amp when 0.5 v is applied. This results in a conductivity $\sigma_2 = 4.8 \times 10^{-12}$ (ohm cm)$^{-1}$ if the film is 3 microns thick.

The tin oxide is about 1 micron thick and has a sheet resistivity of 30 ohms/square. The sheet resistivity is equal to the resistivity divided by the thickness. The conductivity is then $\sigma_1 = 330$ (ohm cm)$^{-1}$.

Evaluating β,

$$\beta = \left(\frac{4.8 \times 10^{-12}}{3.3 \times 10^{2} \times 3 \times 10^{-4} \times 10^{-4}}\right)^{\frac{1}{2}} = 6.97 \times 10^{-4} \tag{16}$$

This value for β results in a deviation from linearity (see Eq. 15) which is completely negligible and a linear potential distribution is assumed for the tin oxide film.

B. TWO-AXIS POSITION SENSITIVE DETECTOR

Two-axis position sensitive detector operation techniques fall into two general categories. The first category is essentially an extension of the single axis dc mode of operation and the second is an ac mode of operation. In the ac mode, the position information is contained in the amplitude and phase of the output signal. Both of these techniques have been investigated in this program.

There are many detector configurations which can be used in both the ac and dc modes of operation. The two configurations which have been evaluated are (1) four separate electrodes around the active area (see Fig. 3), and (2) a continuous electrode forming a closed square around the active area (see Fig. 4). Both of these configurations can be operated in either the ac or dc mode. The continuous electrode configuration has the advantage that the field pattern will theoretically be undistorted over the entire area enclosed by the electrodes. The separate-electrode configuration was used since it is an obvious extension of the single-axis dc configuration. The comparison of the results of each configuration has been significant to the understanding of the error factors involved. It should be noted that the two modes of operation are distinguished by the driving circuitry rather than the detector configuration. In this evaluation, the separate-electrode detectors were operated in the dc mode and the continuous electrode detectors were operated in the ac mode. The principle of operation of each mode is described below.

Using dc fields, the two sensitive axes cannot be energized simultaneously. Instead, a field is applied to the x-axis and the position of the star image in that axis is measured. The x-axis field is then removed, the y-axis field is applied, and the position in the y-axis is determined. The driving potentials are two square waves 180 deg out of phase, which switch from zero to the operating voltage long enough to determine the star position in each axis. One disadvantage is that the position in each axis is not determined simultaneously. For most applications the time between determinations would be negligible.

Another approach which will provide simultaneous two-axis information is to drive both axes simultaneously with ac fields of widely separated frequencies. The output is filtered to separate the two frequencies and the amplitude of each is the position information.

The ac mode of operation is as follows: If the four corners of the continuous external electrode, or each of the four separate electrodes, are driven with equal amplitude sinusoidal potentials so that each driven point is 90 deg out of phase with the driven point adjacent to it, the field pattern generated in the tin oxide will be as shown in Fig. 4. At the center of the detector, the amplitude of the field will be zero, or a null. The equipotential lines are circles concentric with the center of the detector. Circles with larger radii are equipotentials of larger values. A measure of the amplitude of the field at any point is a measure of the radius of an equipotential circle in the tin oxide.

Another unique feature of the field set up in this manner is that constant phase lines are straight lines which radiate from the center of the detector. The 0-deg phase line radiates from the center to the 0-deg driving contact. The same is true of the 90, 180 and 270-deg phase lines. The phase of any point on the external electrode is a linear function of its position relative to the two adjacent driving points. As an example, the 45-deg phase line is a line from the center of the detector to a point in the center of the electrode between the 0 and 90-deg driving points. Phase lines for 0, 45, 90, 135, 180, 225, 270 and 315 deg are shown in Fig. 4.

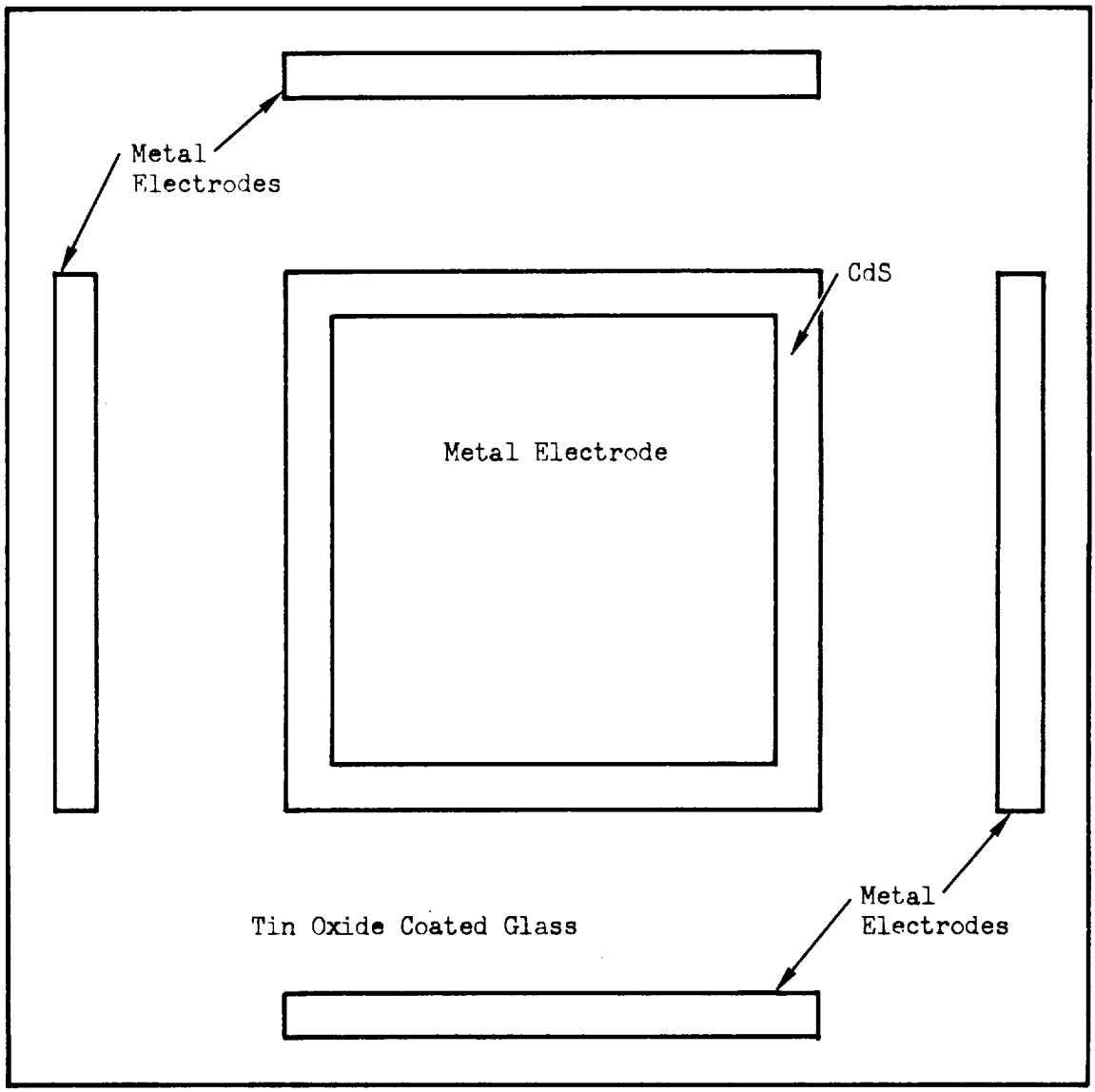

Fig. 3. Two-Axis Separate-Electrode Detector

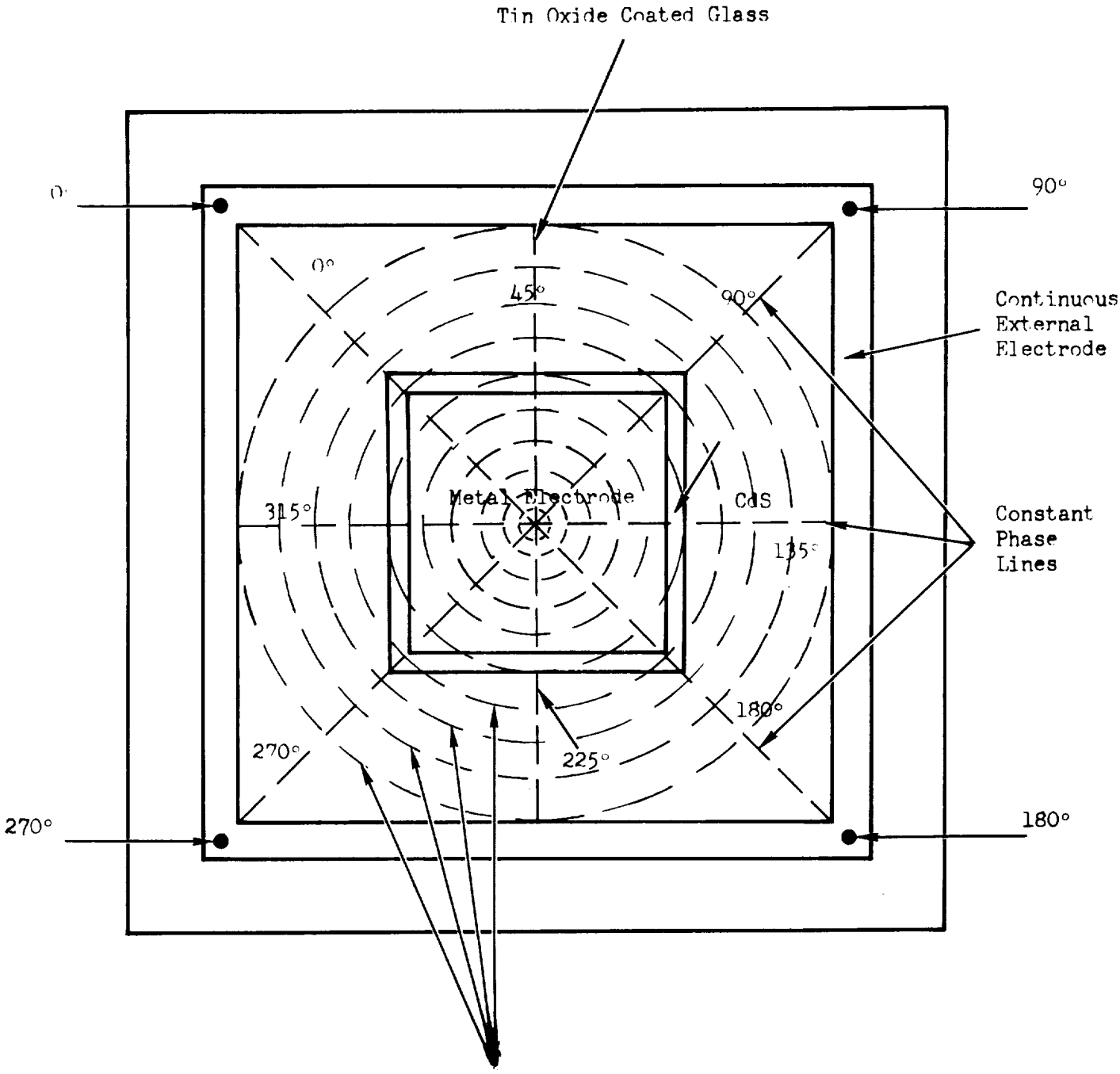

Fig. 4. Two-Axis Rotating Field Detector

With the two-axis ac field, each point in the tin oxide film has a unique value of amplitude and phase. If a star image is present on the active area, the output electrode will take on the potential of the tin oxide at the point of incidence. The amplitude of the output voltage determines the distance of the star image from the center of the detector and the phase of the output determines its position on the equipotential circle. Thus, the output amplitude and phase give the position of the star in polar coordinates where the amplitude is the r vector and the phase is the θ vector.

In both configurations tested, it would have been desirable to extend the active area closer to the external electrodes to prove that the field from the continuous electrode configuration is free from distortion. To expedite the fabrication of the devices so that the evaluation could proceed, this was not done.

IV. PHOTOCONDUCTOR CHARACTERISTICS

The photoconductive material used in the fabrication of volume effect detectors must meet some requirements that are quite different from those for surface effect detectors. The main requirement, due to the fabrication technique, is for a completely continuous and pinhole-free film. Second, the desired photocurrent vs illumination characteristic is very different from that of a surface effect detector. Also, the spectral response of a given photoconductor must be commensurate with the application. In this case, the application of tracking stars of various color temperatures dictates the use of a photoconductive material which is sensitive near the visible portion of the spectrum.

A. MATERIAL CONTINUITY AND UNIFORMITY

It is apparent from the concept of a volume effect photodetector that the photoconductive material between the electrodes should be as thin as possible. Considerations of device impedance and bias voltage values indicate that a practical thickness is about 3 microns. One of the most convenient methods to deposit a film of this thickness is the vacuum deposition method. This technique has a disadvantage in that it is very difficult to vacuum deposit a large-area film which is free from pinholes. It is obvious from the construction of volume effect detectors that any microscopic hole in the photoconductor will allow contact between the two electrodes and cause a short circuit through the device.

The requirement for pinhole-free active material is different from the requirement for surface effect detectors. In the surface effect mode of operation, a very small percentage of the photoconductive film is actually an active detector; therefore, the probability of a pinhole in the active area is greatly reduced. In most cases even if the pinhole lies in an active area, the loss of material is such a very small percentage of the total active material that the effects of the pinhole are insignificant.

A second requirement is the elimination of what may be termed "conductivity holes" through the film. This situation arises when agglomerates of impurities or defects cause microscopic regions of the film to be either highly conducting or insulating. In the case of the highly conducting regions, the detector is essentially short circuited as if a pinhole were present. Small regions of the nonphotoconductive insulating type can be noticed only when that area is illuminated with a small spot lf light, i.e., a star image. Other areas of the detector appear to operate normally. These material problems are the extreme cases of material nonuniformity. Generally, material nonuniformity is a result of an inhomogeneous mixture of the added impurities and the photoconductive film. This gives rise to variations in the photoconductive properties over the surface of the film.

B. PHOTOCURRENT VS ILLUMINATION CHARACTERISTICS

Large area, position sensitive detectors are designed specifically for space applications; i.e., the determination of the position of a star when it is seen with essentially a zero background illumination. Zero background operation requires a very different photocurrent vs illumination characteristic than is required in daylight star tracking. In daylight tracking applications, the detector is required to operate with varying amounts of background illumination and the photocurrent vs illumination characteristic should be linear over the range of illumination levels to be encountered.

Two major requirements in determining the ideal photocurrent characteristic for space operation are (1) the value of the current must be very small when the detector is in a dark state, and (2) when illuminated by a star, the output should not be a function of the star intensity, but only of its position.

The value of the dark current determines the maximum size of the detector. Consider a hypothetical photocurrent vs illumination curve as shown in Fig. 5. The dark current is the result of a current density integrated over the entire surface area. However, the current when a star image is present is a sum of the current through that small area plus the dark current. To achieve a usable output, the current resulting from the area under the star image must be greater than the dark current. In Fig. 5, the left-hand ordinate shows the photocurrent produced by illumination of the entire active area. Assuming a detector that is 100 mil on a side, the active area is 10^4 mil^2. Dividing the photocurrent by the area gives the photocurrent density which is given by the right-hand ordinate. Since the typical star image area is 1 mil^2, the photocurrent density curve also gives directly the photocurrent characteristic for a star image over this illumination range. The total dark current is indicated on the curve to illustrate the illumination necessary for a star to be detected. With a 10^4 mil^2 detector, the star must cause a photocurrent greater than 10^4 times the dark current. Note that the required ratio of star photocurrent to dark current can be lowered by reducing the detector area. Thus, the maximum detector size is limited by the dark current value. Conversely, given a particular detector size and a minimum star to be detected, one can determine the photocurrent characteristic which is required.

The second requirement is that the detector output must be a function only of the star position and not of the star magnitude. This requirement dictates a saturation of the photocurrent characteristic at the illumination level of the dimmest star to be detected. This is also shown in Fig. 5. The state-of-the-art for photoconductive film materials has not yet reached the point where the saturation characteristic can be tailored. Techniques for meeting this requirement will have to be developed in the future.

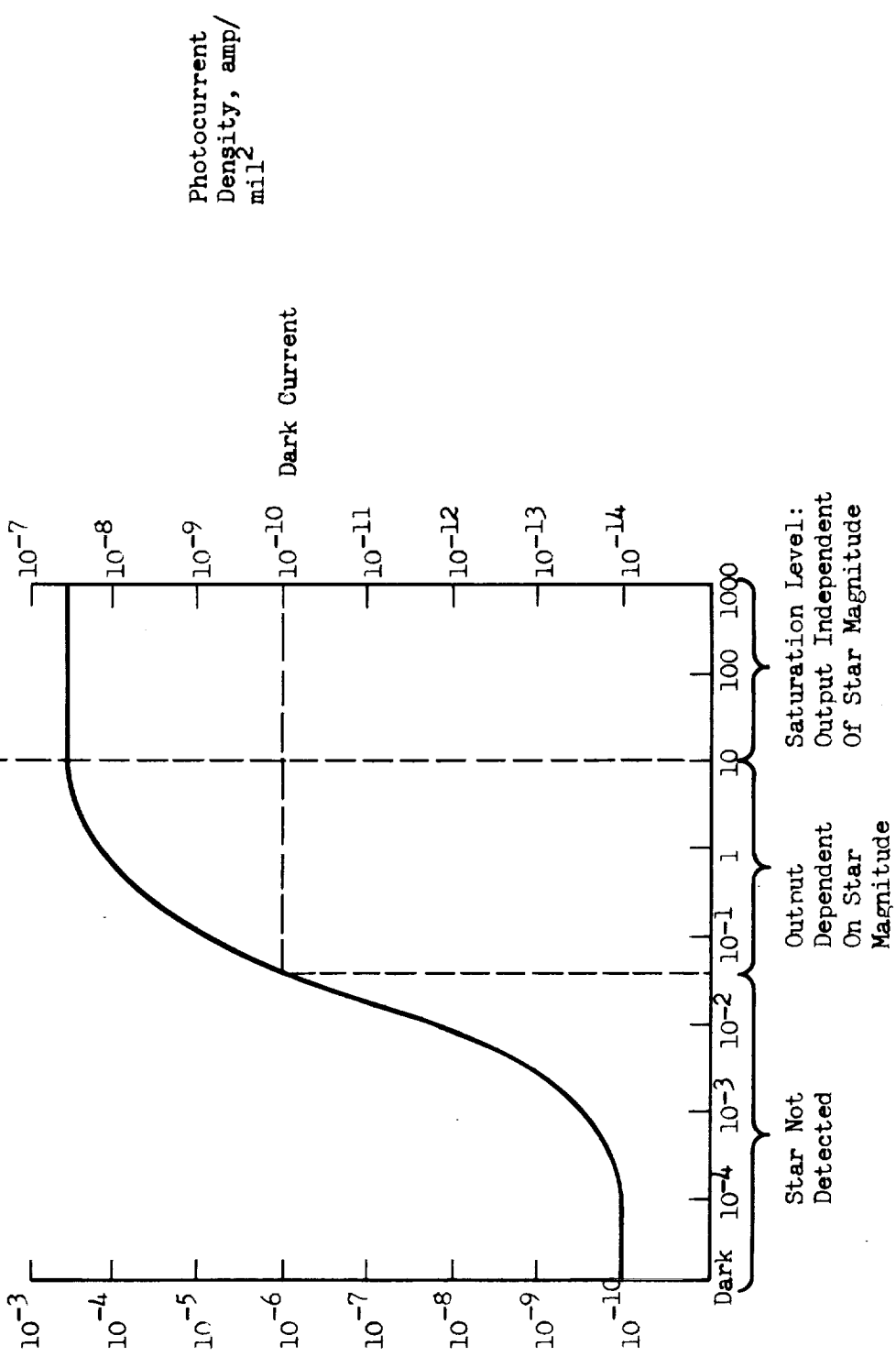

Fig. 5. Hypothetical Photocurrent vs Illumination Curve for 10^4 mil^2 Detector

C. SPECTRAL RESPONSE

In the consideration of a material suitable for photodetectors used in a star-tracking application, the spectral response of the material as well as the areas mentioned above must be taken into account. This is due to the fact that the stars to be tracked are generally of very different colors. The extremes are B-type stars with a color temperature of about 25,000 deg K and M type stars which are 3500 deg K. In analyzing the spectral emission of these stars and star types between these temperature extremes, it appears that the best compromise is to use a material which is sensitive near the visible portion of the spectrum.

Figures 6 and 7 illustrate the measured spectral response characteristics of two of the detectors used in this study. These detectors were fabricated from a vacuum deposited film of cadmium sulfide (CdS) and show the typical response characteristics of this material. The response of CdS is so close to that of the human eye that the usual conversion from visual magnitudes to detector magnitudes is not significant. The visual magnitude can be considered the detector magnitude with little error.

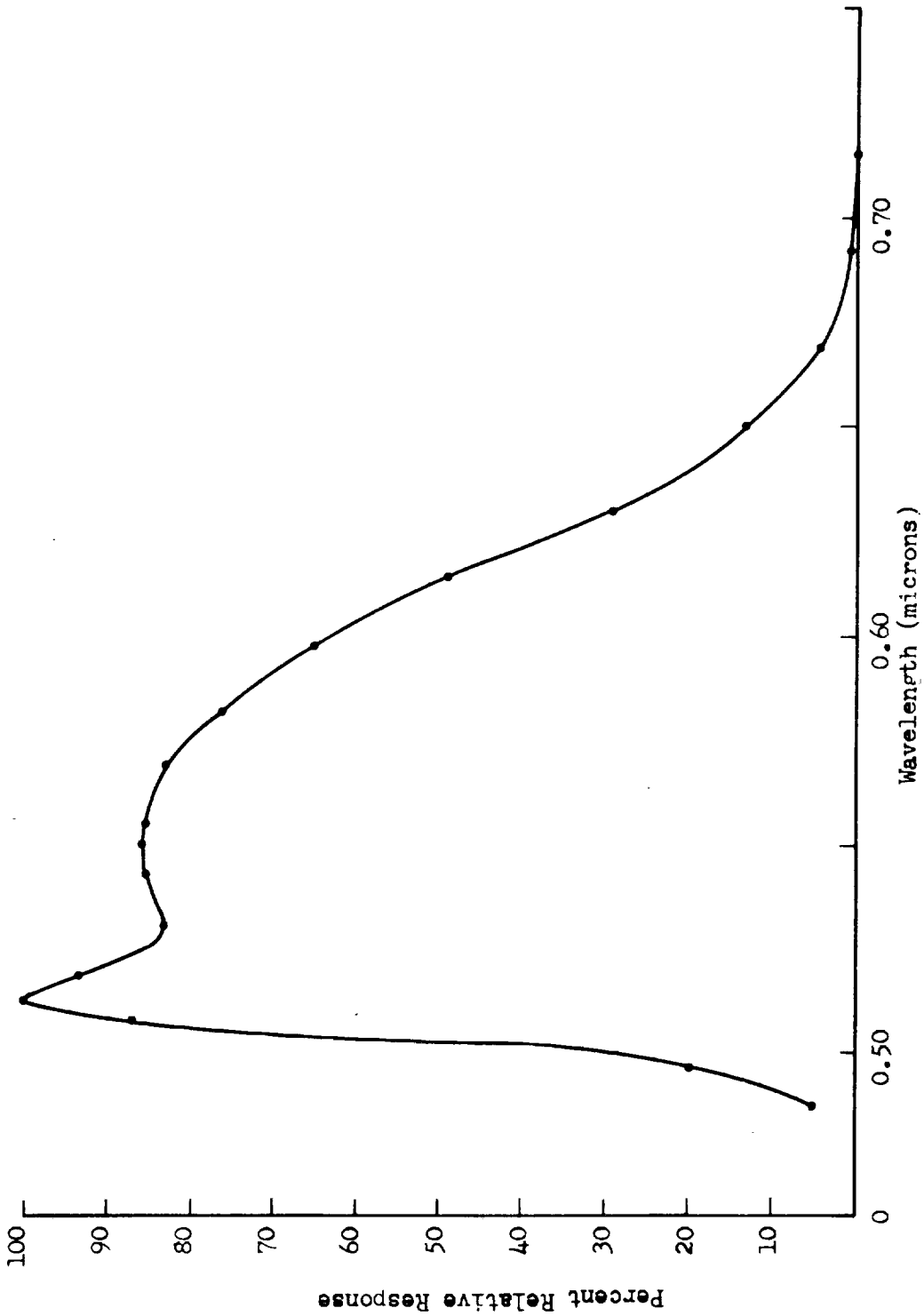

Fig. 6. Spectral Response for Cell No. 1-23-2A

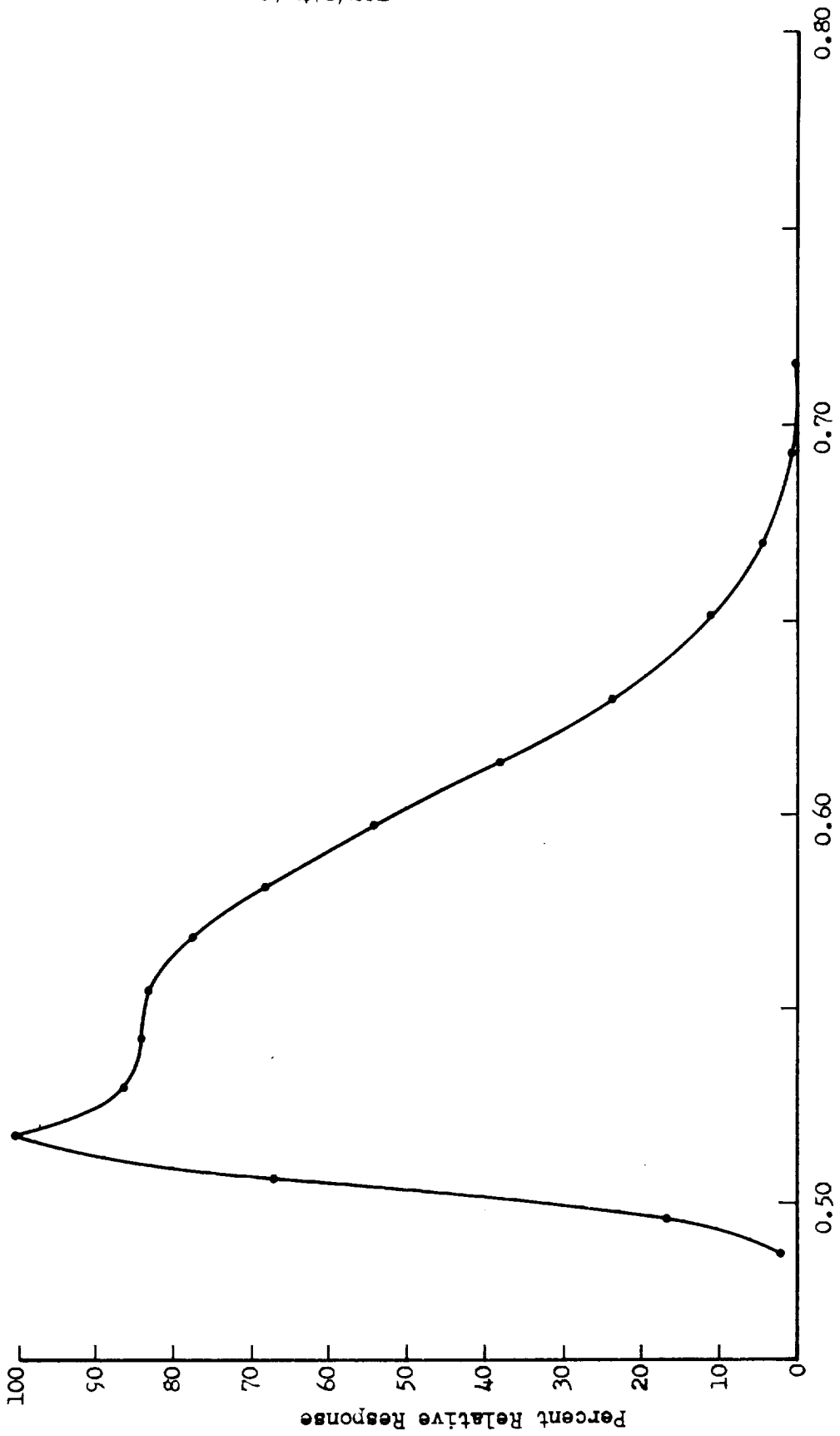

Fig. 7. Spectral Response for Cell No. 1-25-3C

V. DETECTOR FABRICATION

The fabrication of a large area, position sensitive, volume effect detector involves several critical material processes. These processes unfortunately are not independent processes. For example, the results of the diffusion process are a strong function of the parameters of the evaporation process. The results of the electroding process are a function of the material characteristics after the diffusion step. Essentially, all process steps are dictated by the process steps used previously and by those which will follow.

The purpose of this section is to consider in detail the techniques and problem areas in the fabrication of a large area, position sensitive detector since it appears that improvements in these areas are the key to the practicality of these devices.

A. FABRICATION TECHNIQUES

The fabrication of a position sensitive detector consists of nine basic steps. The first step consists of the selection of the basic components, e.g., the glass substrate, the transparent electrode and the CdS material. The glass substrate must have an extremely low alkaline content since diffusion of alkaline impurities into the CdS film destroys the photoconductivity. The glass must also have a thermal coefficient of expansion which is close to that of CdS. If the glass has a very different coefficient of expansion, the CdS film will peel away from the substrate during subsequent processes which require heating. The final requirement for the glass is that its softening point be greater than 600 C since the diffusion process requires heating to this temperature.

The transparent electrode is placed on the glass substrate prior to deposition of the CdS film. The material must be a fairly good conductor (the desired sheet resistivity is approximately 30 ohms/square) and at the same time be transparent to the visible portion of the spectrum. The material selected was tin oxide due mainly to the availability of this material. Considerably more work has been done with tin oxide than other usable materials such as indium oxide or cadmium oxide. Very thin metallic films (sputtered rhodium and platinum) have been tried, but the initial results were not encouraging and these materials were not pursued further. The main problem was that the platinum or rhodium went into either the CdS film or the glass during the diffusion process.

The CdS material used for evaporation is an extremely high-purity material. Mass spectrographic analysis shows it to be in excess of 0.99999 percent pure. Attempts were made to use CdS material which had been doped in the powder form, however, these attempts were not successful since the impurities tended to agglomerate and the resulting film was very nonuniform.

The second step consists of the deposition of the tin oxide film on the glass substrate. The deposition was attempted at Autonetics using a chemical vapor phase deposition technique, however, this process had not yet been completely developed and the results were not considered successful. At the present time, the best approach is to purchase the glass with the tin oxide already deposited. The coated glass used for these devices was obtained from the Intellux Corporation located in Goleta, California. Both the glass and the tin oxide coating were commensurate with the requirements stated above. The one difficulty is that the surface of the tin oxide is quite rough and nonuniform. This surface condition was improved by polishing the tin oxide surface with a 0.1 micron polishing compound.

The third step consists of the deposition of the CdS film. This deposition is an extremely delicate process since the resulting film must be completely free of pinholes and inhomogeneities. The deposition is accomplished by using a vacuum deposition process developed at Autonetics and described in detail in section C.

Probably the most critical of all the processing steps is the diffusion of impurities into the CdS film. Many different techniques have been tried for this process including simultaneous impurity and CdS vacuum deposition, firing of the CdS film and impurities in the high-pressure environment of a bomb, flash evaporation of impurities with the CdS, and planar diffusion techniques similar to those used in silicon technology. The latter technique has given the best results to date.

The next fabrication step is the placing of an electrode on the material so that the material quality may be tested. One of the most desirable characteristics of an electrode is that it forms an ohmic contact to the CdS, so that in the photoconductive process an electron may be replaced in the photoconductor each time one is swept out by the other electrode. In surface effect devices for daylight operation, an ohmic contact is required for the same reason and also since a nonohmic contact will generate noise. It is yet to be determined how large a factor this is in detectors for space applications.

Electroding has been one of the major problems during the course of this study. Many different materials have been tried with unsuccessful results. Most metals apparently diffuse into the CdS film and cause a short circuiting of the device. It was also found that some metals when first deposited on the CdS seem to be satisfactory; however, within a period of several days, the metal apparently diffuses through the CdS with the same effect. It was found immediately prior to the end of the contract period that lead does make a satisfactory contact and seems to stay in place. The devices for which test data are given were fabricated with lead electrodes.

After electroding, the next step is to test the material to determine if the combination of evaporation, diffusion, and electroding processes has resulted in a detector which is of a sufficiently high quality to warrant continuation of the fabrication process. The photocurrent vs illumination characteristic is measured and compared with the requirements developed in section IV.B. If the device meets these requirements the fabrication process will continue; if not, the material is discarded.

The next fabrication step is to etch the CdS film to the required size. The material is etched to the form of a square just slightly larger than the size of the desired active area. The etching is accomplished by standard photo-etch techniques using HCl as the etchant. This particular step has never caused a problem and no devices have been lost at this step.

After the devices are etched, they are ready for auxiliary electrodes to be deposited. These electrodes are used to develop the electric field in the tin oxide film. Initially, chromium was used for the electrode metal, however, it was found that the high temperature required to vacuum deposit chromium caused diffusion of the electrode material into the CdS, thus destroying the device. Lead was subsequently used for auxiliary electrodes so that the temperature of the substrate could be kept below 140 C. The only disadvantage of using lead is that it is not as mechanically strong or quite as adherent as chromium. This factor must be taken into account in handling the completed detectors.

After application of the auxiliary electrodes, the devices are retested to determine if any damage has occurred or whether the photoconductive properties have changed. If the devices pass this test, they are ready for testing of their position-sensitive qualities.

B. PROBLEM AREAS

The major problem areas in the fabrication of a detector have been (1) the determination of correct diffusion times for the required device characteristics, (2) the elimination of transparent electrode-CdS interactions, and (3) the elimination of top electrode-CdS interaction. The problem of determining the optimum diffusion parameters to achieve photocurrent characteristics which are suitable for volume effect detectors will not be described in detail in this report since this work was done on other programs. A detailed description of the process used is included in section C.

The problem of electrode interaction with the CdS film is directly related to the fabrication of these specific detectors and so was included in this program. As discussed above, the tin oxide coated glass was purchased from the Intellux Corporation and little was known of the impurity content of the tin oxide. The effect of impurities was noticed when the CdS photoconductive characteristics were at times degraded during heating for diffusion purposes.

Upon removal of the CdS film from the tin oxide it was found that the sheet resistivity of the tin oxide had increased by an order of magnitude in some cases. This indicated a doping of some type and it was assumed that there was a mutual diffusion of some constituent of the tin oxide into the CdS which was causing the degradation. At this time extremely thin films of sputtered platinum and rhodium were investigated. It was found that the interaction of these films was even greater than when tin oxide was used, and that after a diffusion, approximately 75 percent of the metallic film was gone. The Intellux Corporation was contacted in an attempt to determine the nature of the tin oxide impurities. Because of proprietary reasons, no information was received which would give a clue to the tin oxide impurities. The complete solution of this problem has not yet been found. It was found that by suitable modifications to the diffusion process, the interaction does not always take place. It is not yet known why this difference occurs. It may be a subtle difference in the evaporation process, or it may be due to differences in the tin oxide itself. The devices used for this study program were taken from groups in which the interaction did not take place.

The problem of top metallic electrode interaction was not seen immediately. In the past, indium has been used as a top electrode due to the ohmic nature of the contact. Indium has been used successfully in surface effect devices in the past and initially appeared to be successful. The devices were operable immediately after the indium deposition but would degrade to a short circuit after three or four days. Initially, this shorting was thought to be the result of mechanical damage or of changes in the photoconductor characteristics. It was later found that the indium apparently diffuses into the surface of the photoconductor, thus destroying its properties. Since the photoconductor is only 3 microns thick, a very small amount of diffusion will destroy the device. After this phenomenon was found, many other electrode materials were tested. These included chromium, aluminum, silver, tin, nickel and lead. It was found that the same degradation was apparent with all of these elements except lead. The other elements differed from indium in that the short-circuit mechanism was seen immediately. In the case of lead there is apparently some diffusion, since the photoconductor characteristics are modified by application of the lead compared to what is measured using pressure indium contacts. In fact, the photocurrent characteristics are greatly improved with the lead electrode. It was essentially this breakthrough which has made these devices possible.

C. PROCESS DETAILS

The purpose of this subsection is to describe the actual processes used in the fabrication of volume effect photoconductors.

As mentioned above, the glass substrate is purchased with the tin oxide coating applied. This tin oxide is then polished and cleaned. The cleaning consists of a thorough degreasing and a 1-hr bake at 600 C. Dust or dirt particles on the substrate during deposition are the major causes of pinholes in the vacuum deposited film. After the substrates are cleaned, they are mounted in a cleaned substrate holder which can be closed via a springloaded cover. The substrate holder is then placed in the vacuum system in a closed condition and is kept in this manner until deposition has begun.

The CdS charge is a 0.99999 percent pure material obtained from the Eagle-Pitcher Co. The material is placed inside a specially designed platinum boat so that all evaporation paths are indirect, thus virtually eliminating spitting from the source to the substrate. The dust tight substrate holder is opened only after evaporation has begun and is stabilized. After the holder is opened, the time and the rate of deposition are monitored to result in a film 3-microns thick. The substrate temperature is held at 300 C during the deposition. This process results in a pure and stoichiometric thin CdS film. At this time it is not photosensitive and possesses a very high impedance.

To sensitize the photoconductive film it is necessary to dope impurities in controlled amounts into the film. The process which is used is a modification of a technique reported by Böerr, Esbitt and Kaufman (see Ref. 4.). The CdS samples are placed in a diffusion tube along with a boat containing 8 gm of CdS powder with 1.5 gm of silver and copper placed on top of the powder. The boat is then heated to 600 C while passing N_2 gas through the tube. When the desired temperature is reached, a mixture of N_2 and O_2 gas is bubbled through a container of HCl and passed through the tube for 15 min. After completion, the temperature is held for 5 min more, then lowered. The material is now ready to have lead electrodes deposited and to be tested.

The deposition of the lead electrodes is a straightforward vacuum deposition process. Temperature and time are monitored so that the deposition of the lead electrodes is accomplished in the same manner each time. The testing, etching, further deposition and retesting are accomplished in the manner described in section V.A.

VI. TEST TECHNIQUES

The tests which have been used to evaluate the detectors are of two distinct types. The first test is used to get the basic photocurrent vs illumination curves and the second test is used to interrogate the device with a small spot of light which simulates a star image. The former test employs a calibrated light source operating at 2900 K which is set up so that the entire detector is illuminated. By varying the source-to-detector distance and by using neutral density filters, a range of light levels from dark to 1000 ft-candles can be achieved. The basic detector characteristic is determined by monitoring the current as a function of the illumination. The star simulator is more intricate and is described separately below.

A. TEST FIXTURE

It is necessary to use a test fixture which will hold the detector in place and at the same time make electrical contact with the various electrodes on the detector. To accomplish this, a fixture was built which is illustrated in Fig. 8. Five spring-loaded contact pins were embedded in a Plexiglas block mounted inside a metal box. Two holes were drilled through the Plexiglas block and connected via a small tube to a vacuum pump. When a detector is placed on the test fixture the vacuum holds the device in place. The four corner pins contact the four corners of the auxiliary electrodes, while the center pin contacts the lead electrode on the active area. The light spot is incident on the photoconductor from the top through the glass substrate and the transparent electrode. The one disadvantage of a test fixture of this nature is that the contact positions are not adjustable. In this case the contact positions were fixed with a 0.275 in. separation of the corner contacts with the fifth contact directly in the center of the square described by the corner contacts. This fixture will handle any size of active area from 0.250 in. on a side, to 0.030 in. on a side. The test fixture was found to operate very efficiently and has greatly decreased the time required to take test data. Also, the fixture has virtually eliminated the possibility of damaging a device by mechanical probing.

B. ILLUMINATOR

The illuminator used to simulate a star image consists of a small light bulb which illuminates a pinhole. The light passing through the pinhole is incident on a beam-splitting mirror. One half of the light is focused into a 1.3 mil diameter light spot by a microscope objective lens. The remaining one half of the light is reflected up through an eyepiece. The operator can look through the eyepiece and see the light spot as well as the detector. This arrangement is a requirement for any kind of efficient alignment or focusing technique. The illuminator is suspended above the detector test fixture by a three-axis micropositioner. Each axis can be moved a total of 0.500 in. in increments of 0.0001 in.

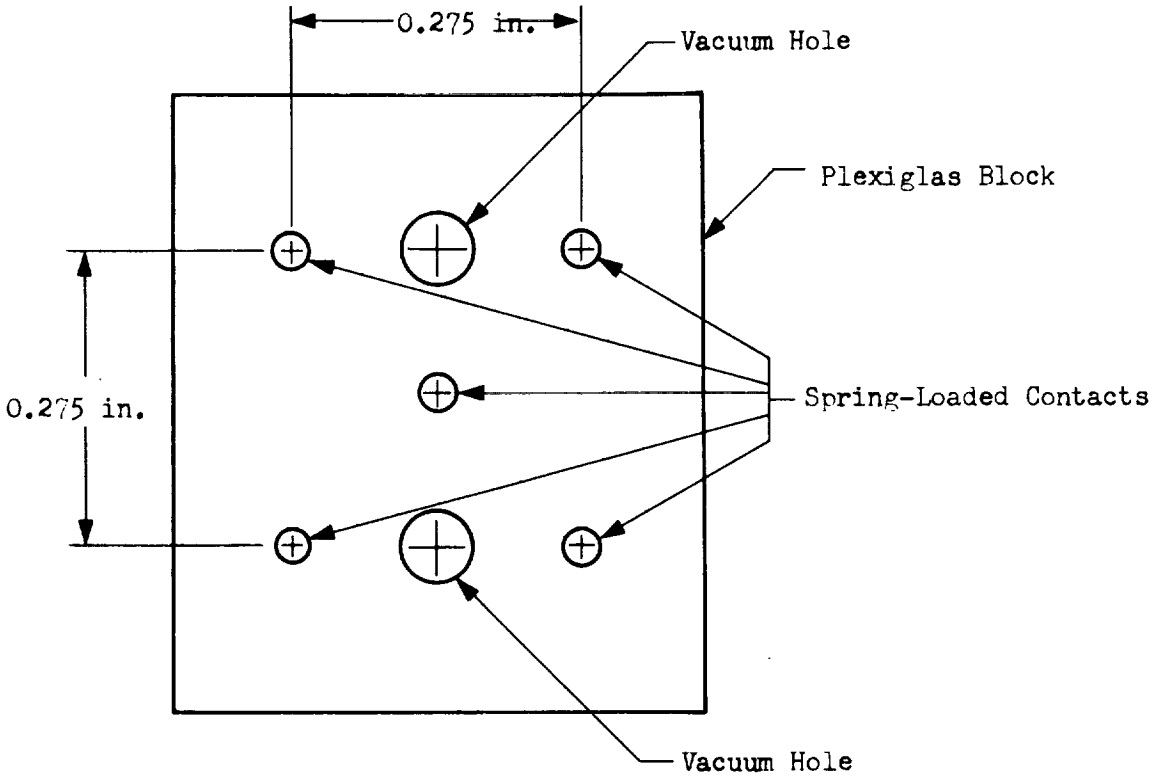

Fig. 8. Test Fixture

C. TEST TECHNIQUES

The test techniques are similar for all tests. The main differences between tests are in the circuitry and in the electrode configuration. In all tests, the detector is placed on the test fixture and the light spot is placed at the edge of the detector in one corner. The light spot is moved in 10-mil increments over the entire area of the device by moving in a line across the device in one axis, then translating the line by 10 mil and moving back across the detector. This movement is continued until the light spot transverses the entire active area of the device. Each test results in 80 to 90 data points for each device.

The sequence of tests for each detector is as follows. First, the photocurrent vs illumination curves are taken. Second, the detector photocurrent uniformity is measured. A 0.5 v bias is applied between the tin oxide film and the top electrode. The light spot, which is maintained at a constant illumination, is moved over the area and the photocurrent is measured at each position. For the third test, the detector is operated as a single-axis, dc position-sensitive detector and the star image is moved over the entire area in the same manner. The final test is a two-axis, position sensitive evaluation. The details of these evaluations and the results are described in the following section.

VII. TEST RESULTS

A detailed experimental evaluation was conducted on five operating position sensitive, volume effect detectors. These tests were conducted at various stages of completion of the detectors. After the photoconductive material had been deposited and sensitized, a lead electrode was deposited and the photocurrent vs illumination characteristics were determined. If these characteristics were satisfactory, two external electrodes were deposited so that the detectors could be operated in the single-axis dc mode of operation. At this stage, all five detectors were tested for single-axis position accuracy. Following this test, the detectors were completed by deposition of the remaining external electrodes. Of these five detectors, three were tested with continuous electrodes and two with separate electrodes.

A. PHOTOCURRENT VS ILLUMINATION CHARACTERISTICS

The detectors evaluated are identified by the numbers 1-23-2A, 1-25-3C, 1-25-3D, 2-1-1C, and 2-1-2C. These numbers indicate the evaporation and diffusion runs from which they came so that the history of each device can be traced completely through all processes. All five devices are similar in that they use pure CdS as the photoconductive film and all have the same active area. The active area is the area of the lead electrode on top of the CdS film. In all cases, this area is approximately 90 by 90 mil. The external electrodes are 30 mil wide and are separated by 275 mil center-to-center. Initially, the external electrodes were chromium; however, this material was later changed to lead when it was found that the heat required for chromium deposition damaged the photoconduction properties of several detectors. Lead can be deposited to the same sheet resistivity value as chromium and the deposition process requires much less heat.

The data in Fig. 9, 10, 11, 12, and 13 were taken with a 0.5 v bias between the tin oxide and the top lead electrode. The detector was illuminated by a calibrated light source and the photocurrent measured by a micro-microammeter in series with the detector and the bias supply.

The photocurrent data were converted to photocurrent density in amp/mil^2 by dividing by the active detector area. The photocurrent produced by a star image can be read directly from the curve, since the image area is approximately 1 mil^2. Illumination values for stars of +2.5 to -5.0 visual magnitude were calculated and shown in the curves, as well as the dark current level.

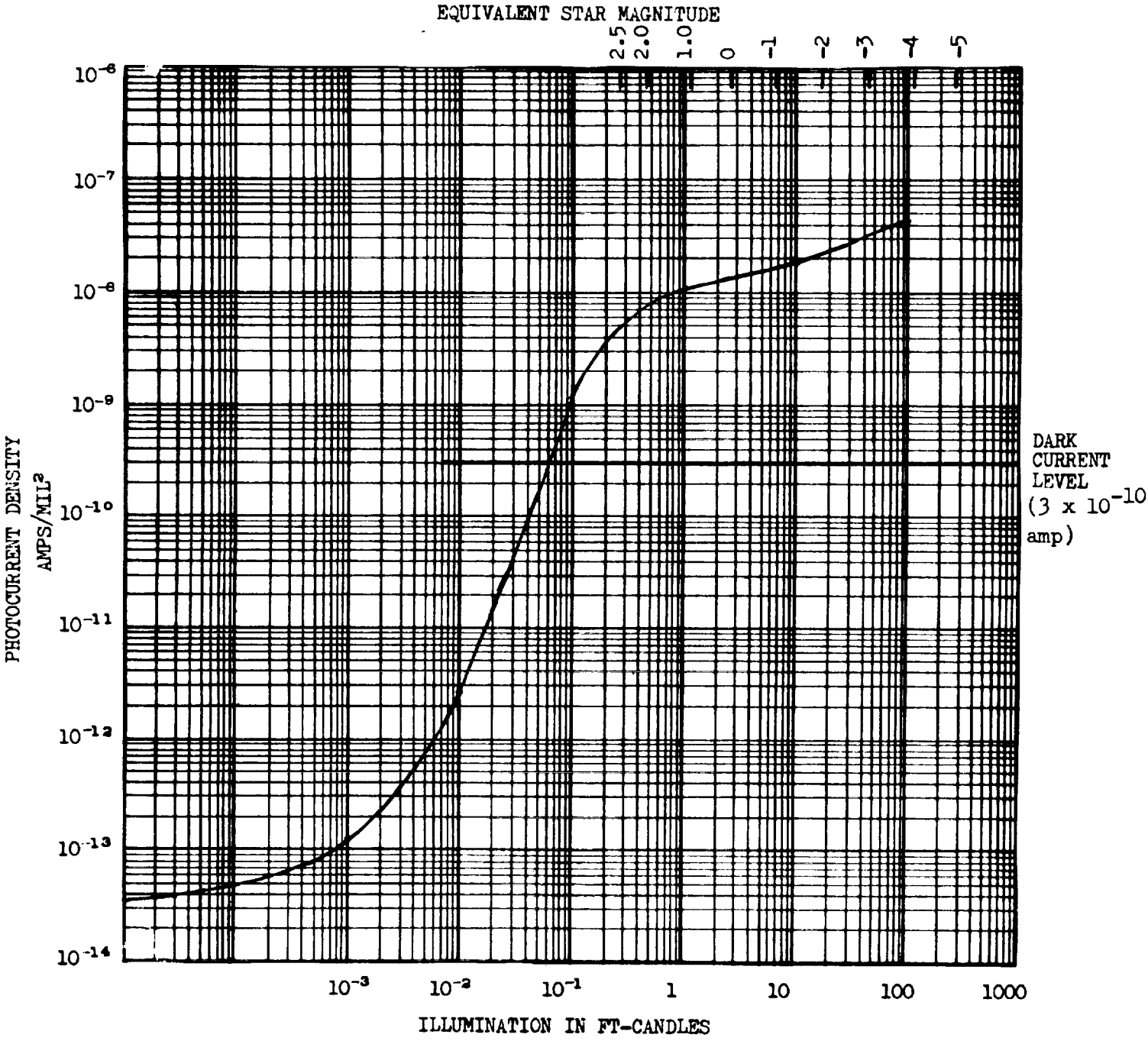

Fig. 9. Photocurrent vs Illumination Curve for Cell No. 1-23-2A

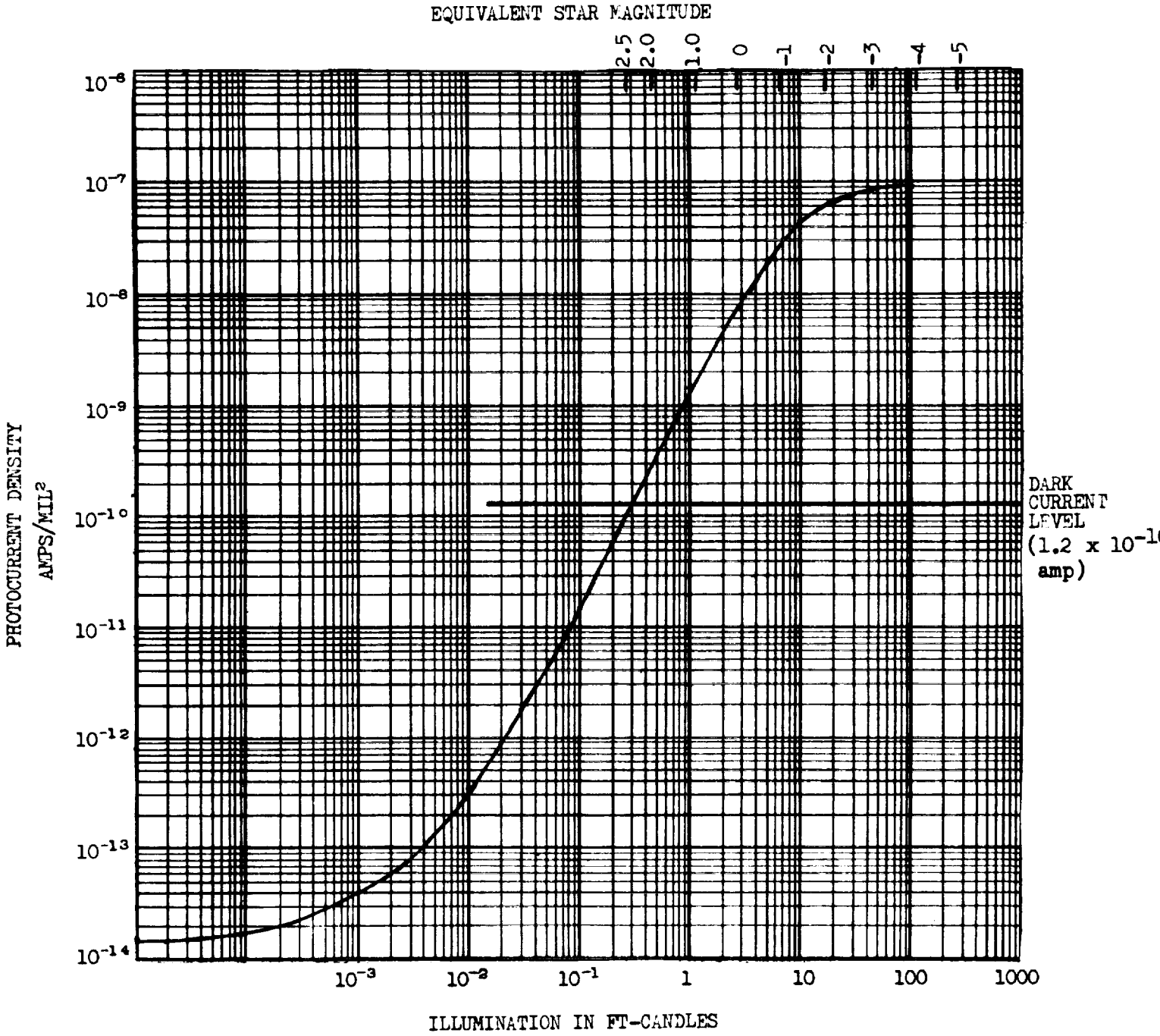

Fig. 10. Photocurrent vs Illumination Curve for Cell No. 1-25-3C

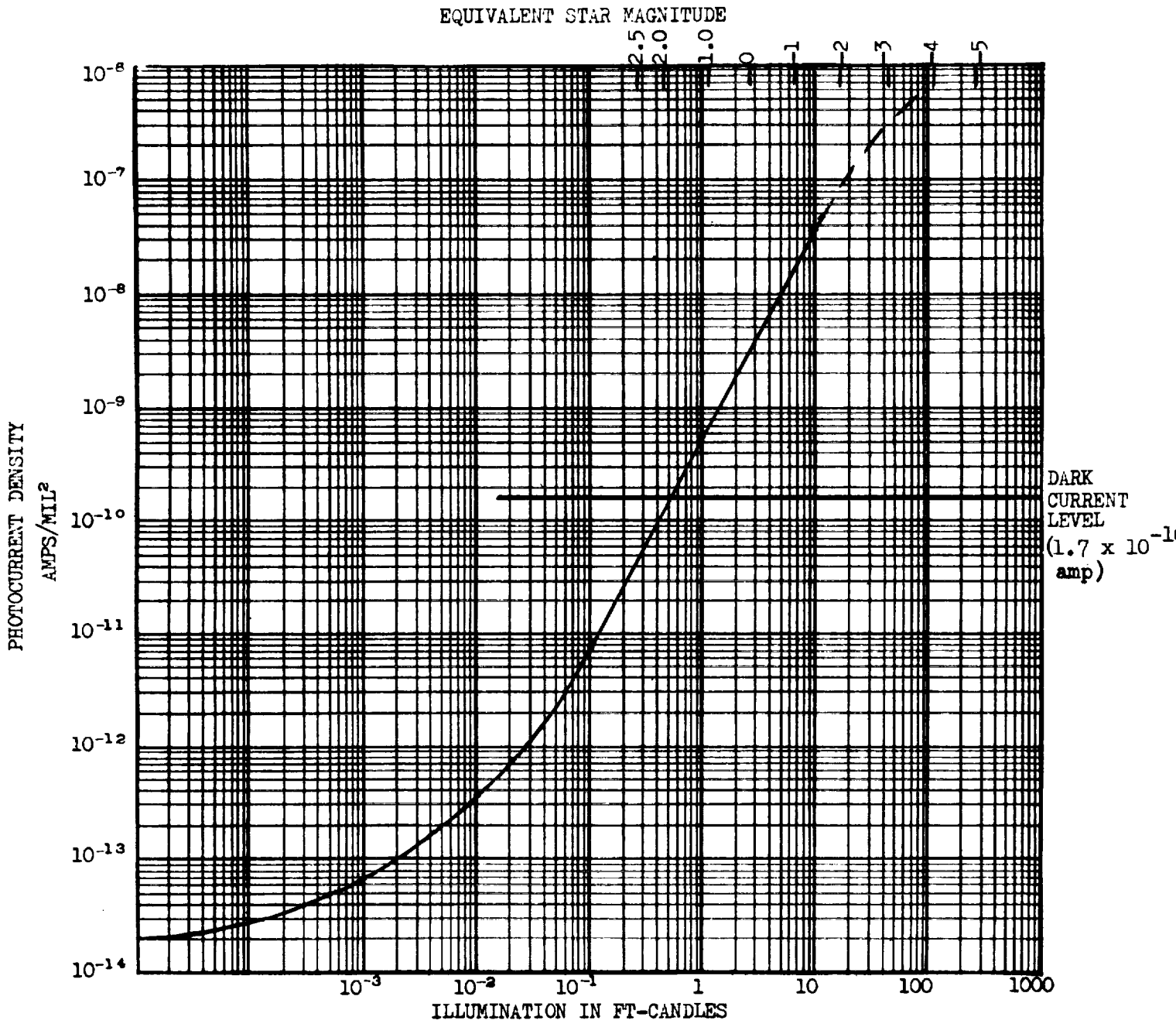

Fig. 11. Photocurrent vs Illumination Curve for Curve No. 1-25-3D

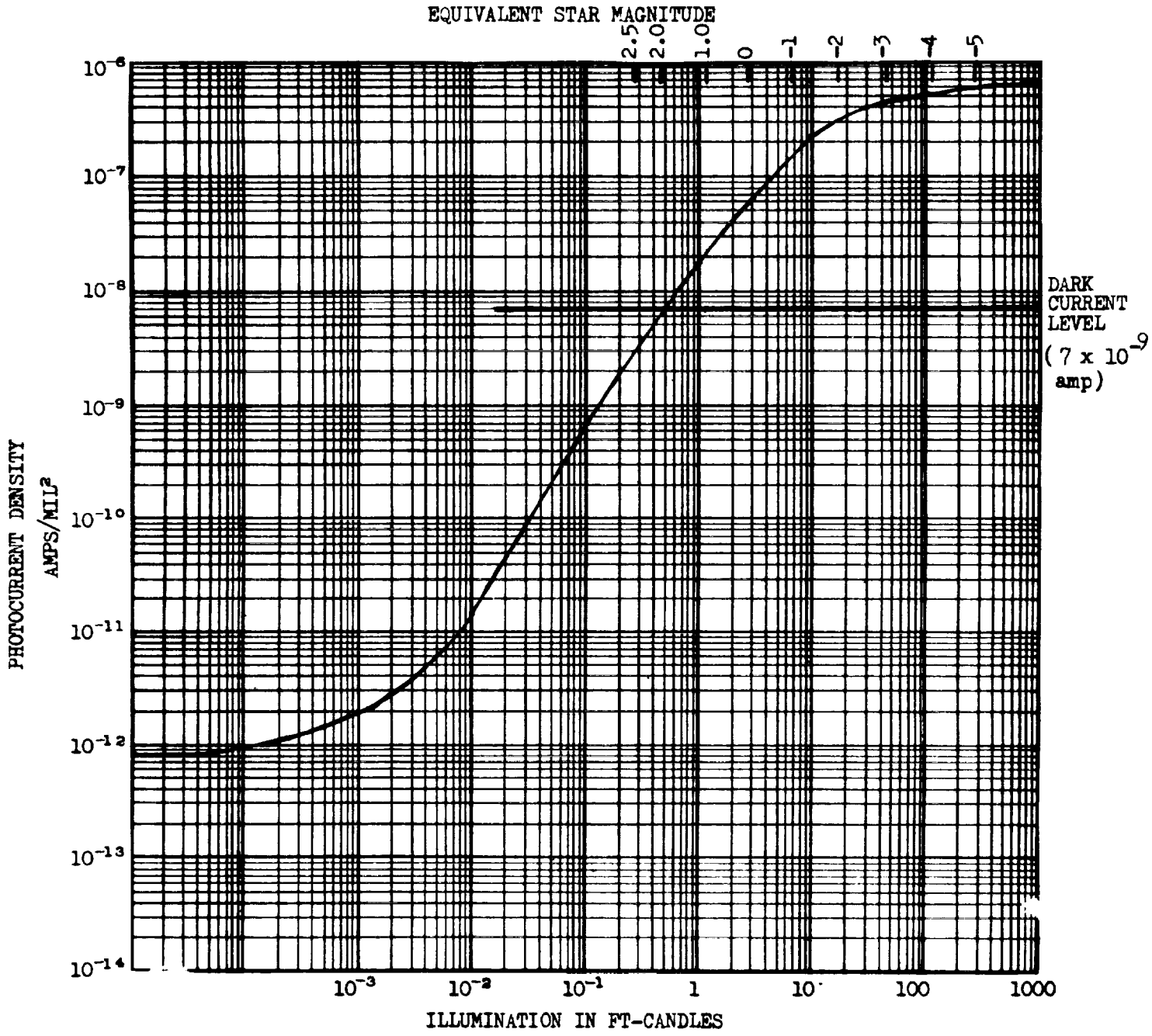

Fig. 12. Photocurrent vs Illumination Curve for Cell No. 2-1-1C

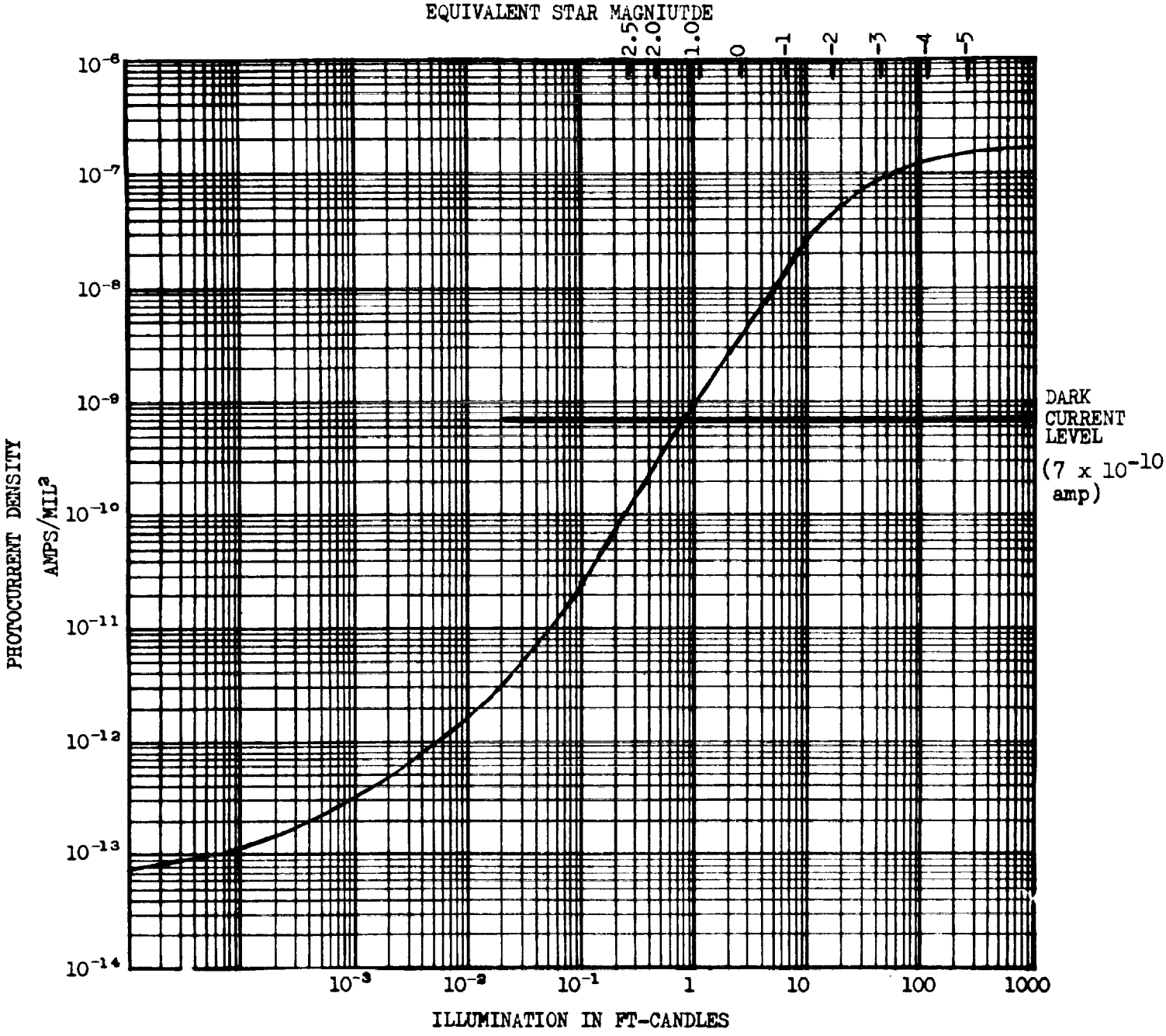

Fig. 13. Photocurrent vs Illumination Curve for Cell No. 2-1-2C

Only one detector (1-23-2A) has a dark current level less than all star currents down to +2.5 m_v. The star current from a +1 m_v star lies above the dark current level in all cases. The +2.0 m_v star is above the dark level in two cases.

One discrepancy which has not yet been resolved appears in the comparison of this and later evaluations. Detectors 1-23-2A and 2-1-2C when illuminated by a star image of about -2.5 m_v had star currents of just over 1 x 10^{-6} amp. This current is higher than would be expected from the characteristic curves. The explanation of this may be that the saturation condition which appears at high light levels when the detector is uniformly illuminated does not take place with a point source illumination. This may be due to a high sheet resistivity of the tin oxide films or a high contact resistance which might have a current limiting effect at high illumination levels.

B. DETECTOR UNIFORMITY

Detector photocurrent uniformity was measured by connecting all four external contact points (see section 6.C) together to one side of a bias supply. The other side of the supply was connected through a micro-microammeter through the center contact point to the lead electrode on the active area. The bias supply voltage was maintained at 0.5 v. The point source illuminator was set to an illumination level approximately equivalent to a -2.5 m_v star. This illumination value was held constant throughout the test. The light spot from the illuminator was 1.3 mil in diameter. The photocurrent was recorded each time the light spot was moved an increment of 10 mil.

The uniformity data are given in Tables 1 through 5. The average value of the star current is given at the bottom of each table, as well as the standard deviation of the individual photocurrents from the average value. With the exception of detector 2-1-2C which had a standard deviation of 5.75 percent, the values ranged from 11 to 21 percent. No correlation has been determined between the standard deviation and the photoresponse of the detectors. Detectors 2-1-2C and 1-23-2A had the highest star current values of the five, but one was the most uniform and the other the most non-uniform of the group.

It will be seen that those detectors having good uniformity when output current is measured (as in this section) are not necessarily the most uniform detectors when output voltage is measured. The detectors which showed the best two-axis position uniformity had standard deviations of 5.75 and 17.7 percent.

C. SINGLE-AXIS DC MODE

Single axis dc evaluation was performed on all detectors after application of the first two external electrodes. The circuit used for this test is shown in Fig. 14. The voltage between the external electrodes was maintained at 1-v dc. The output voltage was measured with a Kintel Model 605 voltmeter having an input impedance of 10^{14} ohms. With the two external electrodes only, the

Table 1. Photocurrent Map of Cell No. 1-23-2A

0.50	0.84	0.84	0.87	0.84	1.15	1.00	0.90	
0.80	1.20	1.17	1.10	1.15	1.20	1.20	1.15	0.82
0.80	1.15	1.27	1.30	1.36	1.10	1.37	1.20	0.82
0.79	1.13	1.31	1.32	1.45	1.35	1.50	1.27	0.74
0.81	1.14	1.37	1.37	2.00	1.40	1.40	1.30	1.10
0.81	1.20	1.38	1.37	1.60	1.40	1.35	1.33	1.15
0.92	1.20	1.49	0.66	1.41	1.57	1.35	1.15	1.10
0.93	1.20	1.40	1.42	1.20	1.55	1.56	1.40	1.20
0.92	1.20	1.30	1.21	1.45	1.46	1.40	1.33	1.15
0.91	0.99	0.92	1.20	0.92	1.30	1.25	1.10	

All currents x 10^{-6} amp
Average current 1.18 x 10^{-6} amp
Standard deviation 20.8 percent

Table 2. Photocurrent Map of Cell No. 1-25-3C

2.00	1.60	1.70	1.40	1.10	1.40	1.40	1.20	1.00
1.70	1.40	1.60	1.40	1.50	1.70	1.40	1.40	1.40
2.00	1.50	1.30	1.40	1.50	1.50	1.60	1.50	1.50
1.50	1.50	1.40	1.30	1.60	1.50	1.70	1.40	1.40
1.50	1.40	1.40	1.50	1.50	1.50	1.70	1.40	1.30
1.60	1.60	1.30	1.50	1.50	1.50	1.80	1.70	1.50
1.70	1.50	1.40	1.40	1.50	1.50	1.70	1.30	1.50
1.40	1.60	1.40	1.70	1.50	1.60	1.60	1.40	2.40
1.50	1.60	1.30	1.90	1.50	1.40	1.40	1.50	1.40
1.50	1.60	1.40	1.70	1.70	1.70	1.40	1.50	1.50

All currents x 10^{-8} amp
Average current 1.51 x 10^{-8} amp
Standard deviation 11.1 percent

Table 3. Photocurrent Map of Cell No. 1-25-3D

1.00	1.00	0.94	0.85	1.00	1.15	1.05	0.96	1.15
0.92	1.00	1.00	1.05	1.00	1.30	1.00	1.10	1.15
0.98	1.00	1.05	1.10	1.00	1.10	1.10	1.10	1.25
0.96	1.00	1.20	1.00	1.20	1.10	1.30	1.15	1.10
1.00	1.10	1.10	1.10	1.10	1.10	1.05	1.20	1.20
1.00	1.00	1.15	1.00	1.20	1.05	1.10	1.00	1.00
1.00	1.10	1.15	1.00	1.10	1.10	1.10	1.40	1.00
0.90	1.02	1.10	1.10	1.10	1.15	1.10	1.05	1.10
0.42	1.05	1.20	1.20	1.20	1.30	1.00	1.00	1.05
0.20	0.86	1.00	1.00	1.15	1.10	1.00	1.20	1.10

All currents x 10^{-8} amp
Average current 1.07 x 10^{-8} amp
Standard deviation 14 percent

Table 4. Photocurrent Map of Cell No. 2-1-1C

1.3	3.0	3.6	4.0	3.1	2.8	3.2	4.4	4.2
3.7	3.3	3.6	3.6	3.1	3.3	3.3	4.2	3.9
3.5	3.7	5.4	3.5	4.2	4.8	3.9	4.9	5.4
4.8	3.8	3.8	3.6	3.5	5.2	4.4	3.2	5.1
3.8	4.2	3.3	3.8	5.0	3.3	4.0	3.8	5.0
4.0	3.4	3.2	3.5	4.0	3.4	3.5	4.7	4.5
3.1	4.8	4.2	4.2	3.8	3.1	3.0	4.3	4.4
3.9	4.1	3.7	4.6	5.0	3.7	3.4	3.4	3.4
3.0	3.4	3.7	3.8	4.7	3.9	3.5	3.5	2.9

All currents x 10^{-7} amp
Average current 3.84 x 10^{-7} amp
Standard deviation 17.7 percent

Table 5. Photocurrent Map of Cell No. 2-1-2C

1.00	1.00	1.09	1.11	1.05	1.10	1.08	1.05	1.10
1.08	1.11	1.01	1.05	1.10	0.80	1.02	1.12	1.05
1.05	1.00	1.02	1.12	1.12	1.08	1.05	1.10	1.08
1.05	1.00	1.05	1.09	1.12	1.05	1.10	1.03	1.15
1.10	1.00	1.10	1.13	1.05	1.08	1.10	1.05	1.05
1.12	1.06	1.15	1.10	0.80	1.12	1.12	1.10	1.12
1.14	1.11	1.12	1.10	1.10	1.20	1.10	1.10	1.10
1.07	1.13	1.10	1.16	1.10	1.10	1.12	1.10	1.20
1.10	1.10	1.11	1.10	1.12	1.12	1.12	1.10	

All currents x 10^{-6} amp
Average current 1.08 x 10^{-6} amp
Standard deviation 5.75 percent

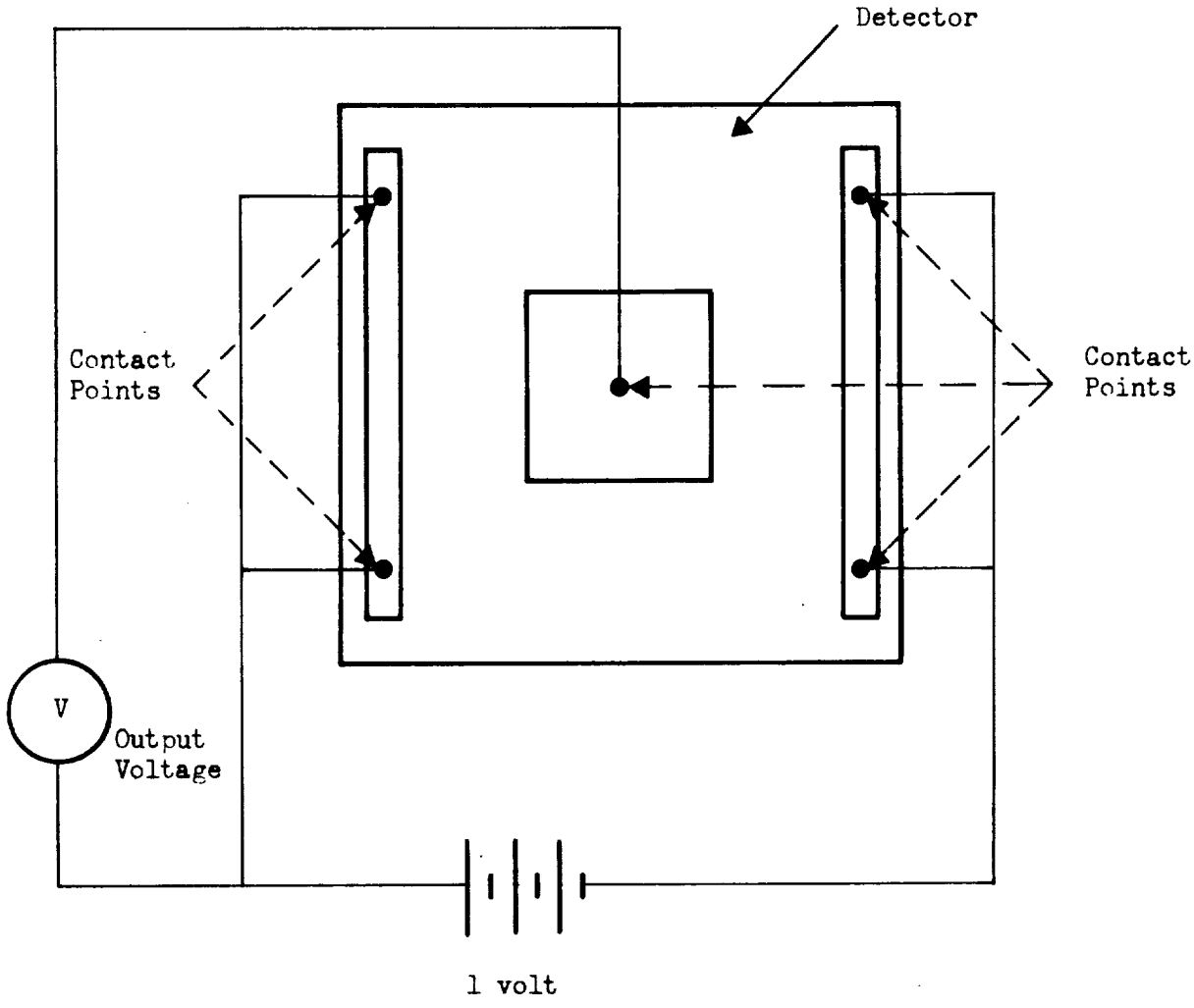

Fig. 14. Single-Axis DC Circuit Configuration

equipotentials under the active area should be equally spaced straight lines. The position sensitivity data were taken by moving the 1.3 mil diameter light spot, equivalent to about a -2.5 m_v star, across the detector in 10 mil increments as was done for the uniformity measurements. The output voltage was recorded at each point and the data plotted in Fig. 15 through 19. Equipotential lines were drawn by interpolating between the data points. The data from the five devices vary substantially in quality. Detector 2-1-2C gave the most accurate position information with a maximum error of 4 mil. Detector 2-1-1C was quite uniform but showed a skewed effect particularly at the bottom right corner. Detector 1-23-2A showed the same type of skew and had an extreme distortion along the left side. Detectors 1-25-3C and 1-25-3D, the two detectors which previously had displayed much lower star current levels than the other three, appeared to show deviation from linearity approaching 10 mil in the extremes. The position sensitivity of detectors 1-25-3C, 1-25-3D, and 1-23-2A was approximately 1 millivolt/mil, while detectors 2-1-1C and 2-1-2C showed 3 millivolts/mil of star position.

A point of particular interest is that the single-axis dc tests do not correlate with the photocurrent uniformity tests. In the photocurrent uniformity test, the resistance of the illuminated photoconductor was measured. In the position sensitivity test, the resistance of the photoconductor is always much less than the input impedance of the voltmeter, which makes the nonuniformities in the resistance of the photoconductive material negligible.

Later tests have indicated that the cause of the skew effect in two of the detectors was a result of contact resistance between the contact points and the external electrode.

D. SEPARATE ELECTRODE CONFIGURATION

Following the completion of the single-axis dc evaluation, two more external electrodes were deposited on each detector. Two detectors were selected for evaluation in the separate electrode configuration. The two detectors selected were Nos. 1-23-2A and 2-1-2C. The external electrodes were shortened to the configuration of Fig. 3. Data were taken from these two devices in the same manner as the single-axis evaluation. The same circuit and equipment were used and the star image was the same size and intensity. A 1-v bias was applied between the two opposite electrodes and the output voltage was measured as a function of star position. After the data were completed from one axis, the bias voltage was applied between the other two external electrodes and the same measurements were made.

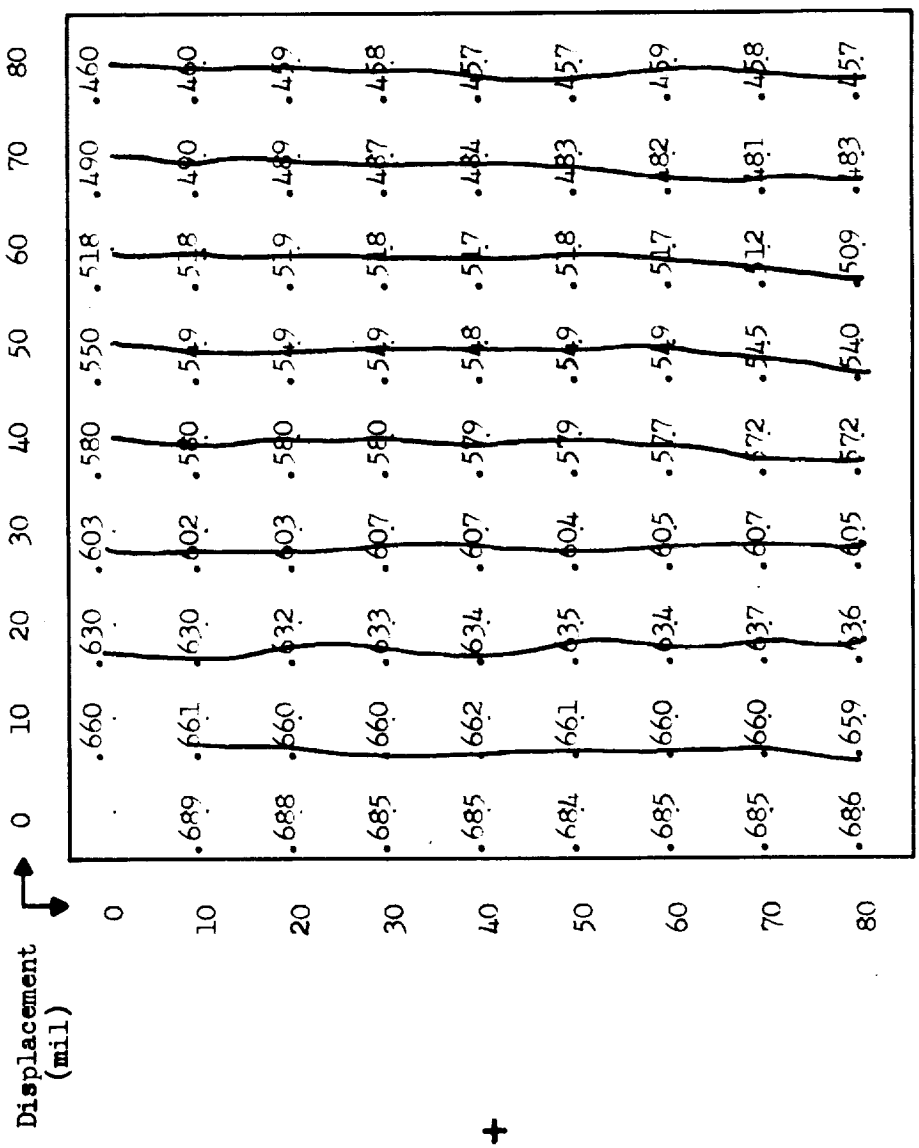

Fig. 15. Single-Axis Position Data, Detector 2-1-2C

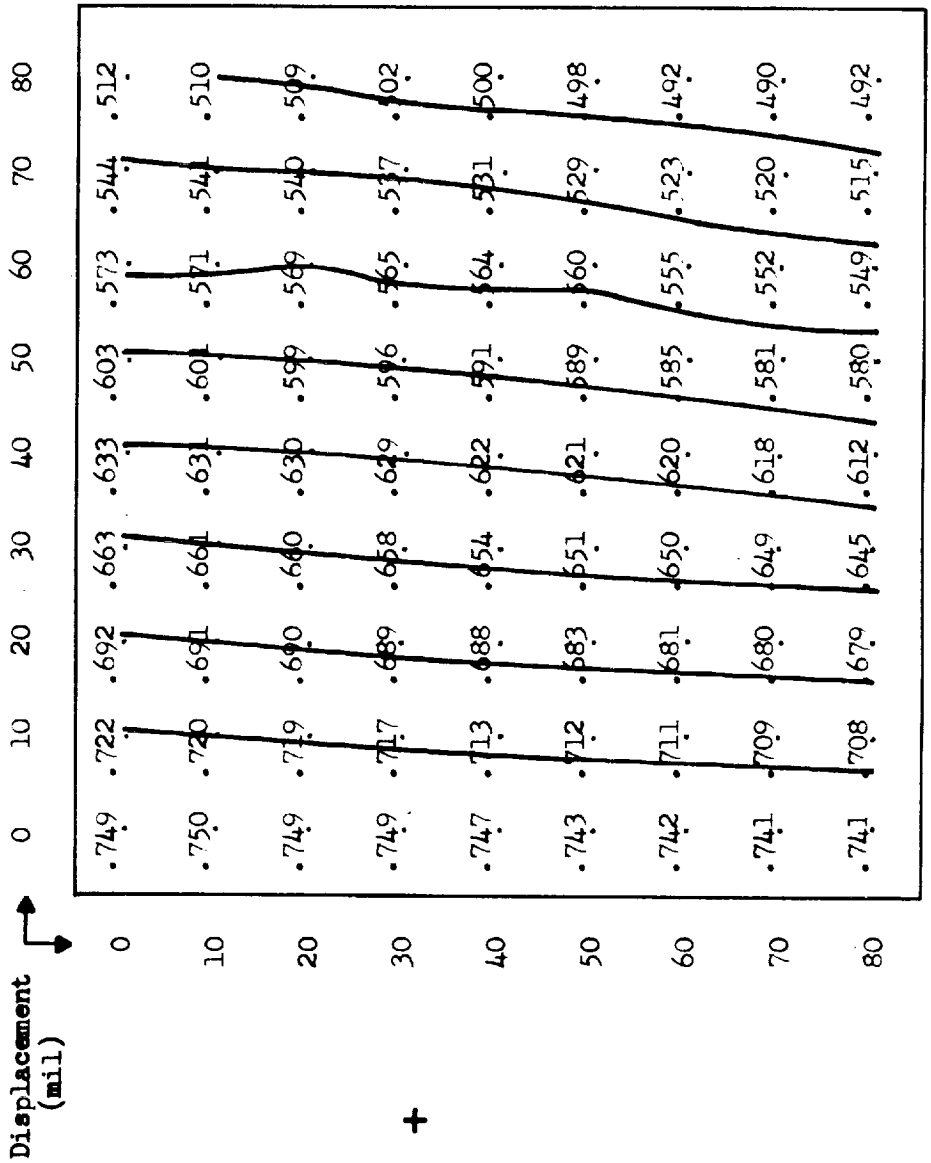

Fig. 16. Single-Axis Position Data, Detector 2-1-1C

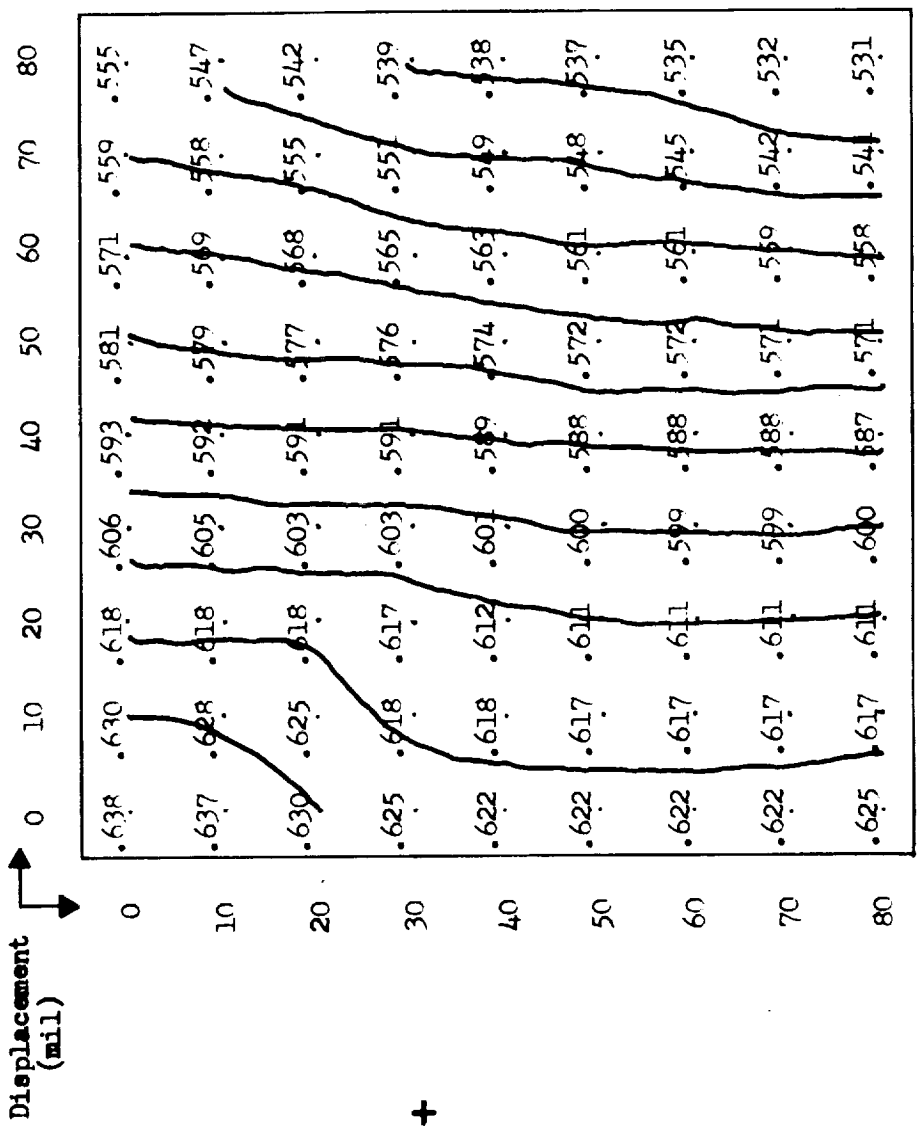

Fig. 17. Single-Axis Position Data, Detector 1-23-2A

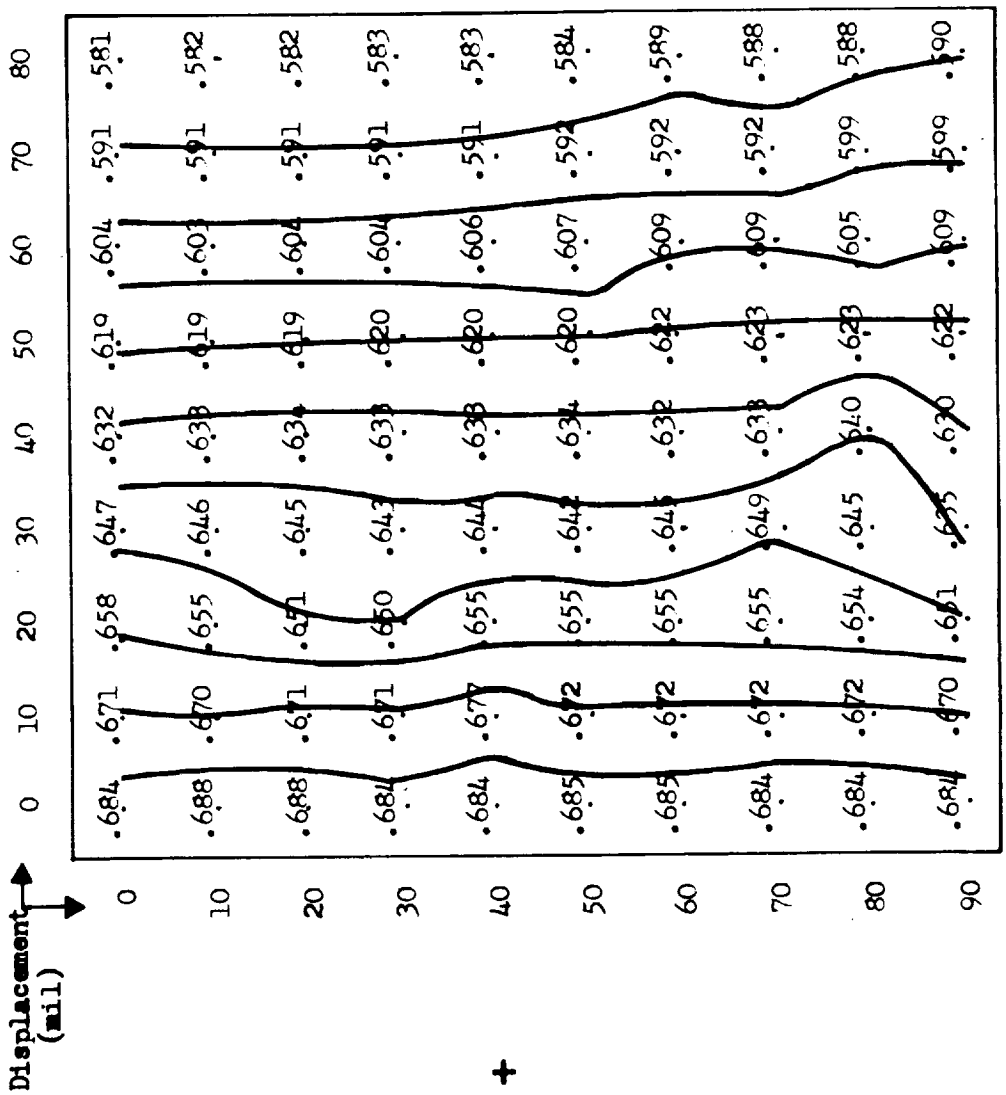

Fig. 18. Single-Axis Position Data, Detector 1-25-3D

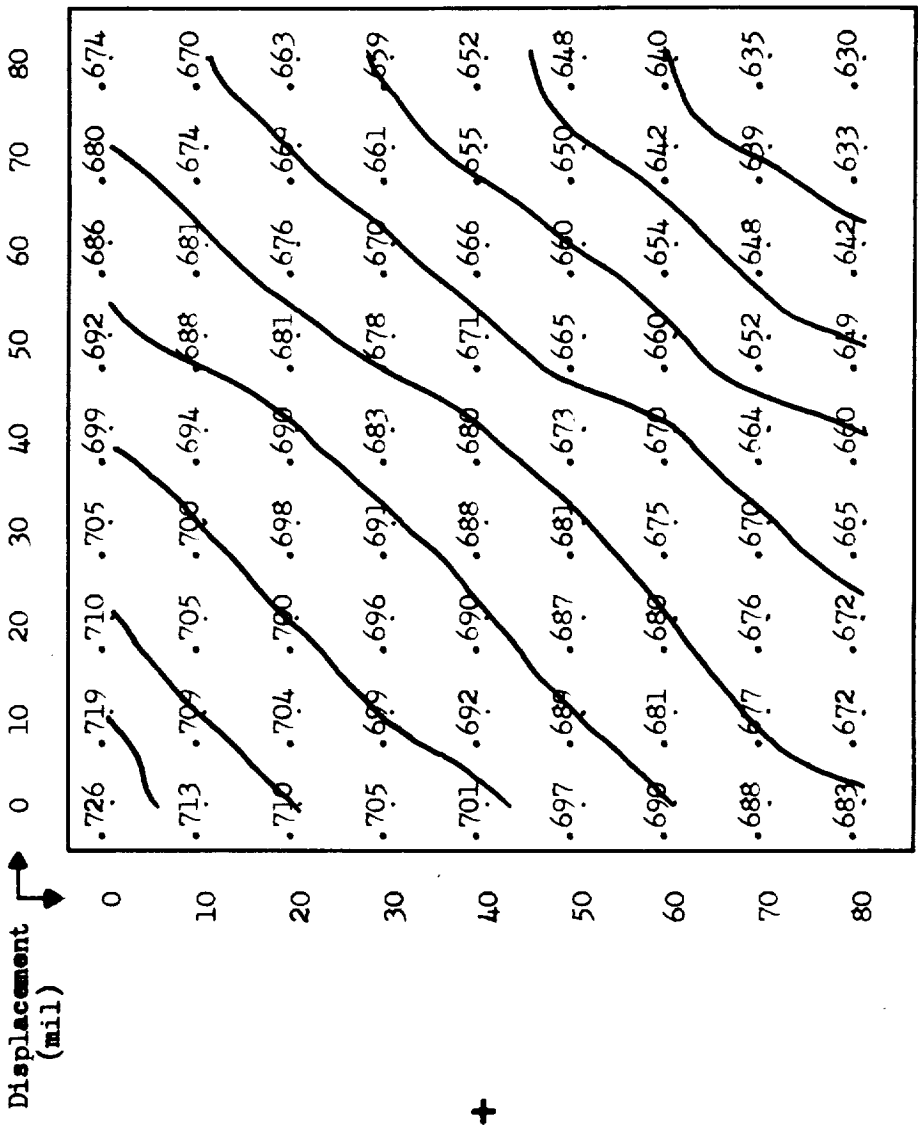

Fig. 19. Single-Axis Position Data, Detector 1-25-3C

The data for both axes of detector 2-1-2C are shown in Fig. 20 and 21. The effect of the second pair of external electrodes is immediately evident. Figure 20 shows significant warping of the equipotentials at the extremities of the active area. The position sensitivity is 3 mv/mil at the right side of the device and increases to 4 mv/mil at the left side. The equipotential lines are distorted as much as 5 mil at the edges of the detector. Figure 21 shows generally the same type of edge distortion as well as a slight skewing of the equipotential lines. The skewed effect must be assumed to result from the field in the tin oxide rather than in the CdS film since the impedance of the CdS is negligible compared to the input impedance of the voltmeter.

Figures 22 and 23 show the data taken from detector 1-23-2A and the data are similar to those of detector 2-1-2C. Essentially the same conclusions can be drawn from this device as from the former. Figure 22 shows the same edge distortion as well as an extreme distortion at the top edge. Figure 23 shows a more uniform equipotential characteristic with more spreading at the top edge than at the bottom. Since complete correlation cannot be achieved between the data from each axis, it appears that the major distortion occurs in the generation of the field in the tin oxide rather than in the coupling of the potential through the CdS.

E. CONTINUOUS ELECTRODE CONFIGURATION

Detectors 1-25-3D, 1-25-3C, and 2-1-1C were evaluated in the continuous electrode configuration. The four-phase driving potentials were obtained from the circuit shown in Fig. 24. Two outputs were taken from a sinusoidal signal generator operating at 40 cps. The two outputs were shifted in phase +45 and -45 deg, respectively. After amplification, the two channels were converted to four-phase, equal-amplitude outputs by the transformer. The readout circuitry is shown in Fig. 25. The output from the center contact point goes to an amplifier with a gain of 1 and an input impedance of 10^{14} ohms, used for impedance matching from the detector to the phase meter and oscilloscope which have an input impedance of 1 megohm.

Since some of the results from previous tests indicated that contact resistance between the contact point and the external electrodes may have been a problem, the resistance of each contact was determined prior to recording the data. In some cases a good contact was not achieved, lending support to the possibility that contact resistance may indeed have caused the error in previous tests.

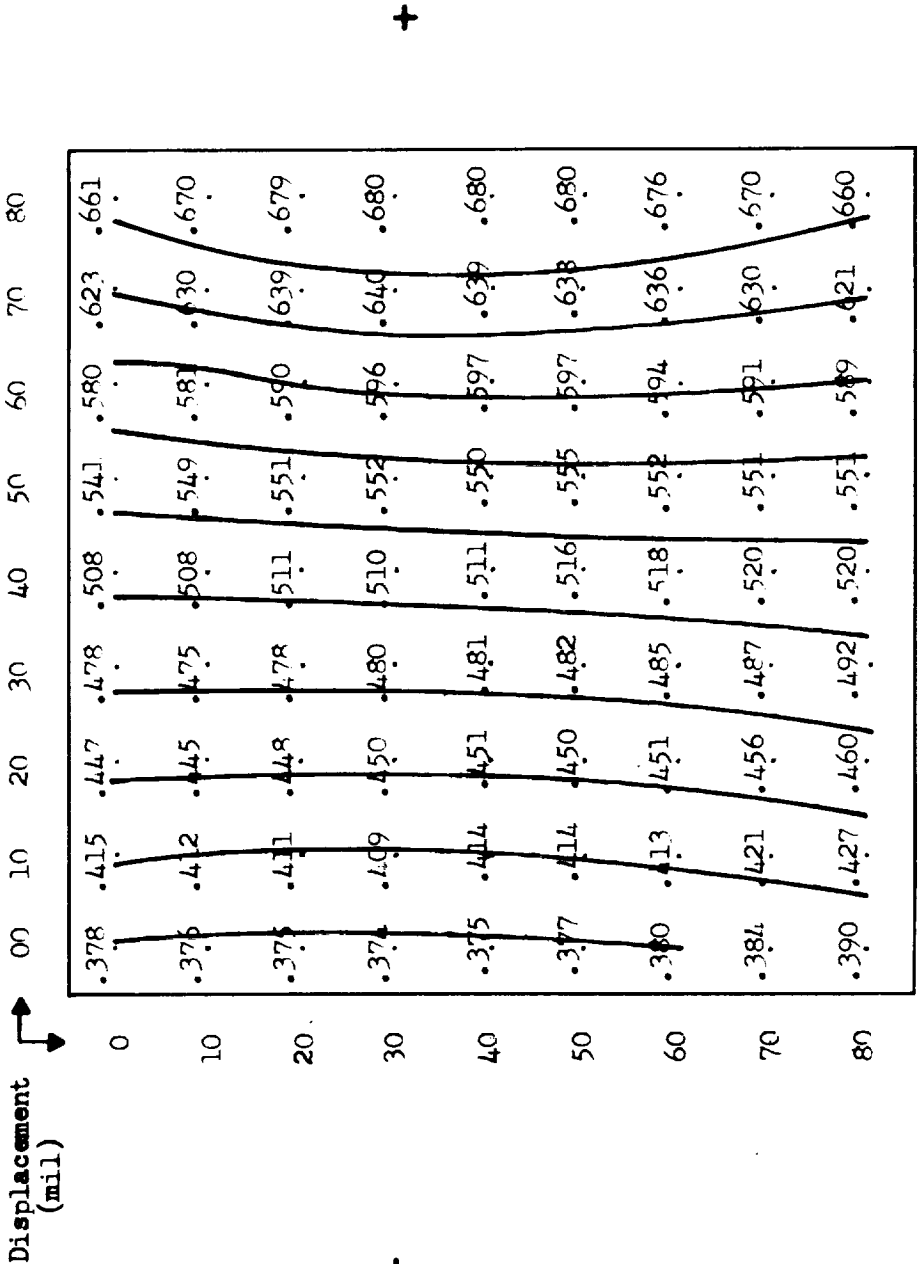

Fig. 20. Single-Axis Four-Electrode Data, Detector 2-1-2C

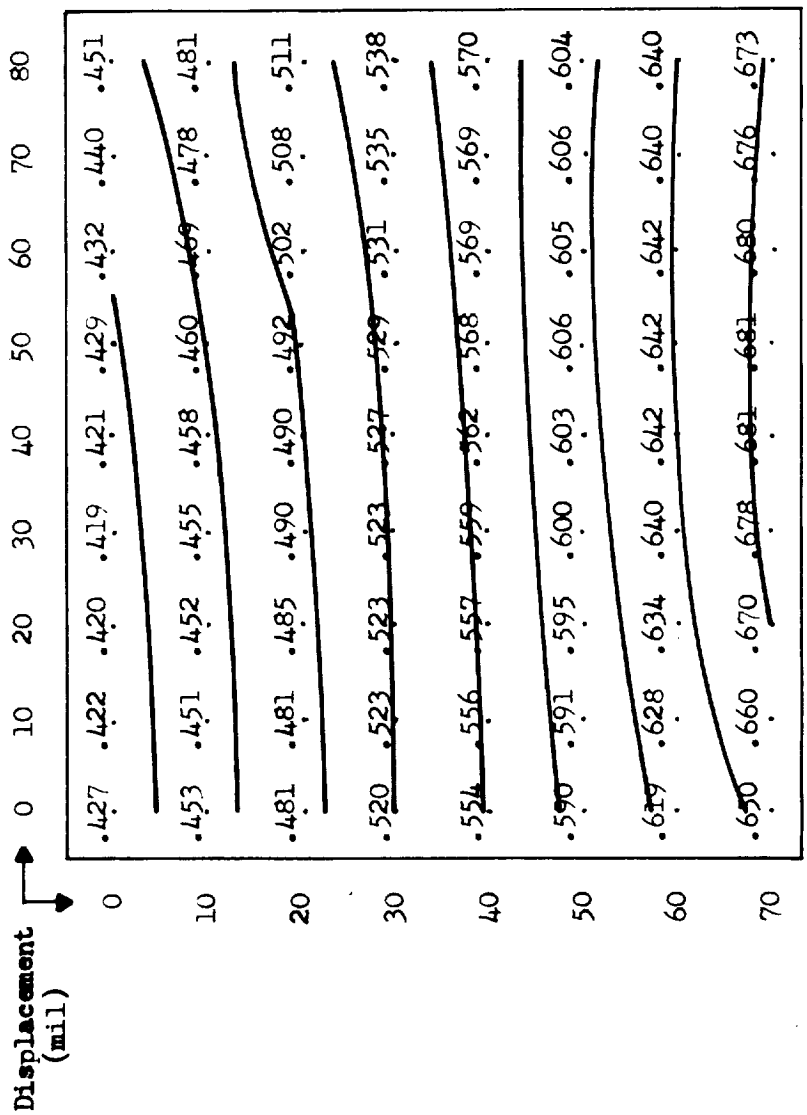

Fig. 21. Single-Axis Four-Electrode Data, Detector 2-1-2C

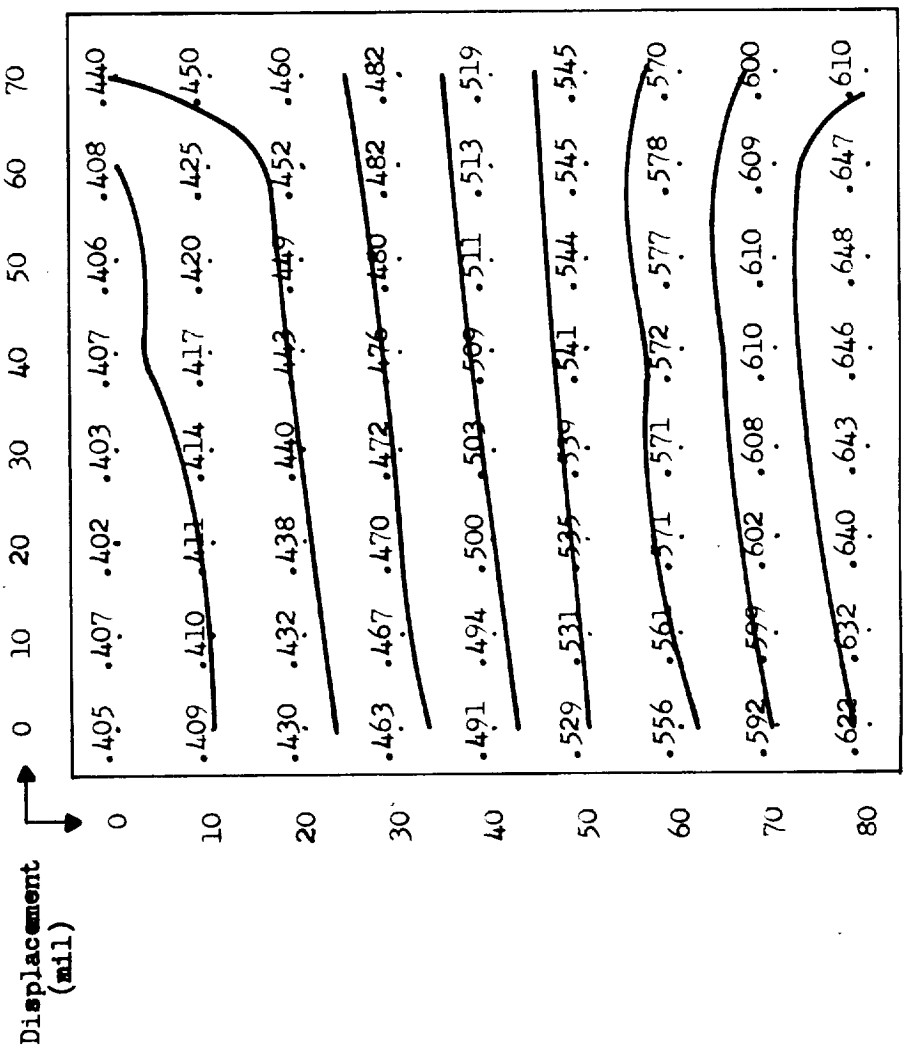

Fig. 22. Single-Axis Four-Electrode Data, Detector 1-23-2A

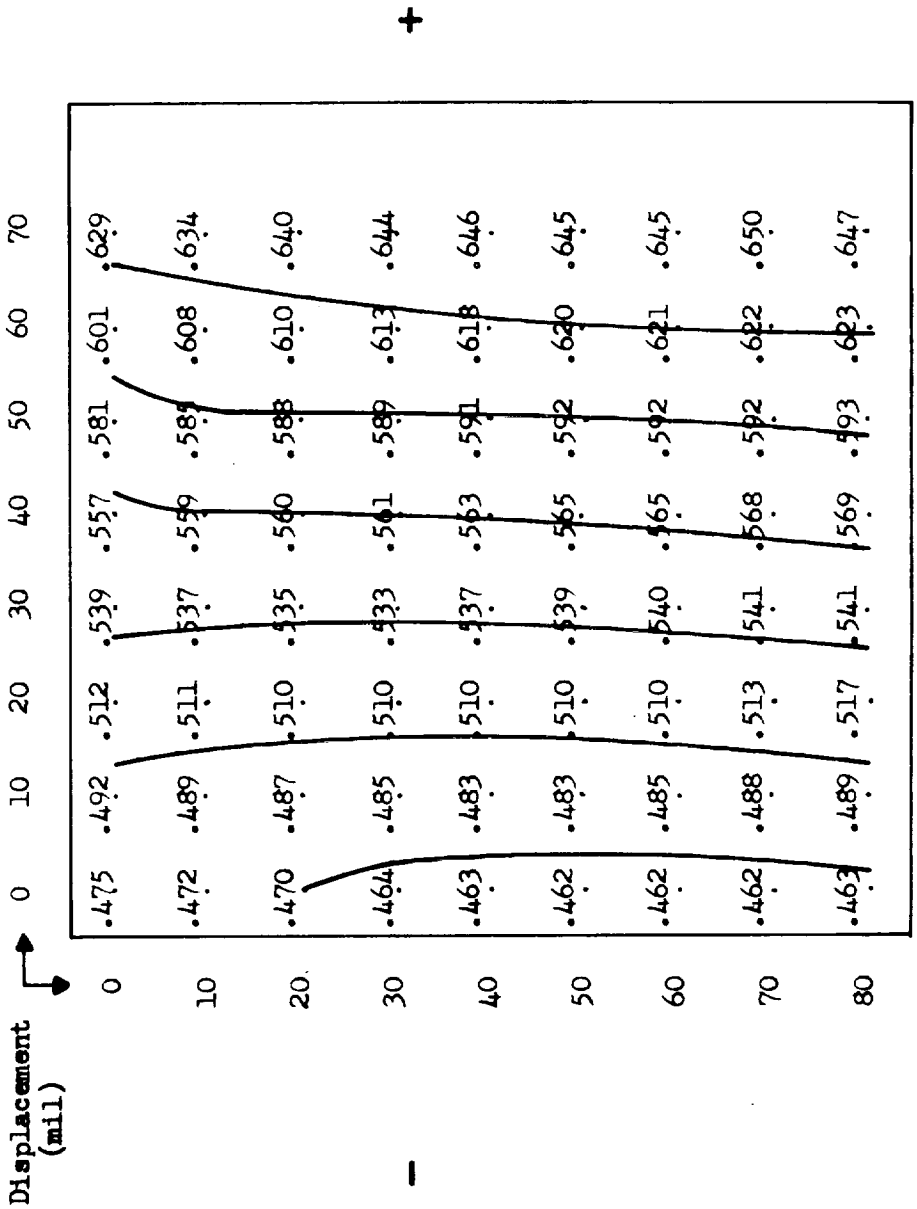

Fig. 23. Single-Axis Four-Electrode Data, Detector 1-23-2A

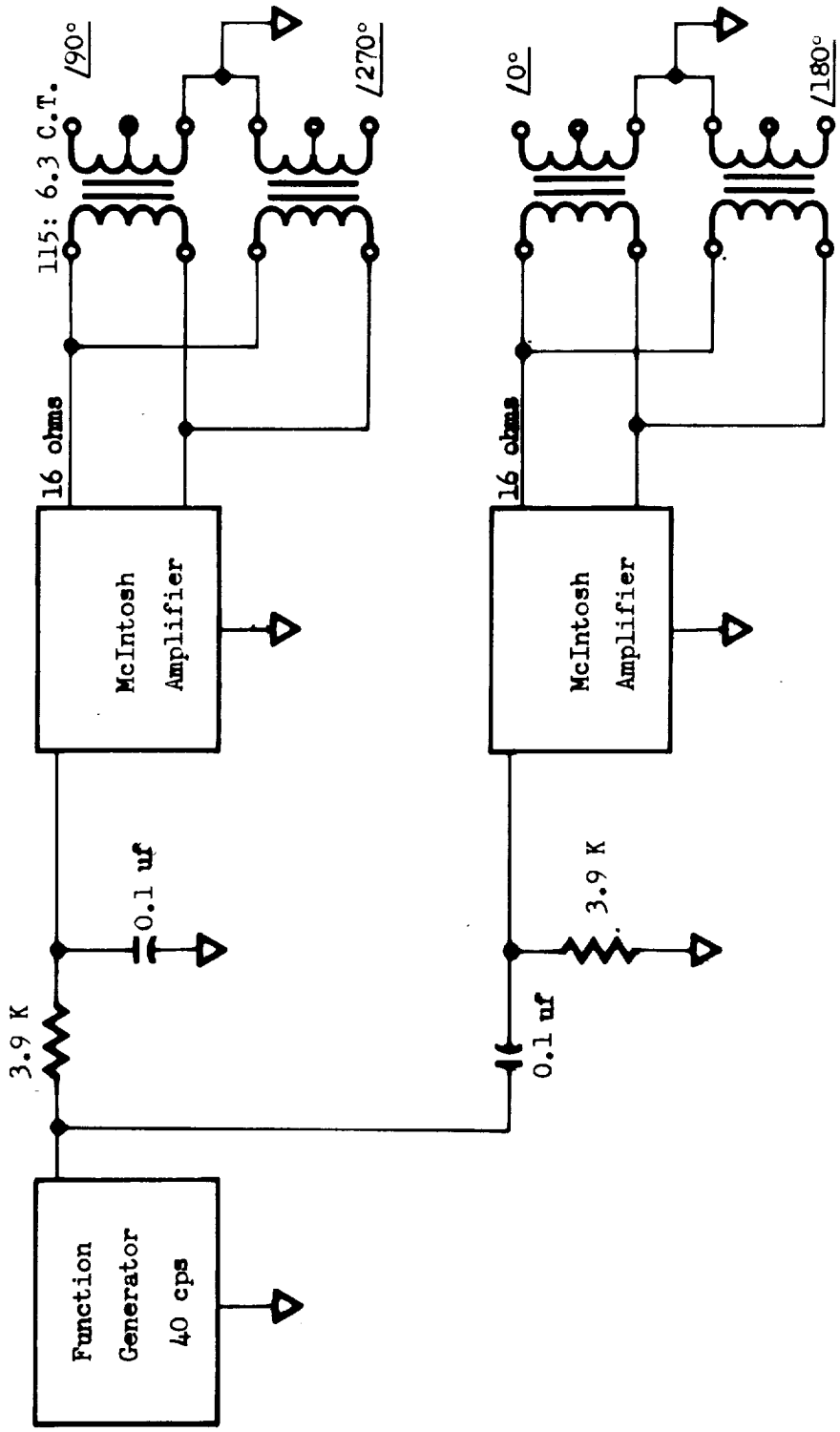

Fig. 24 Driving Circuitry

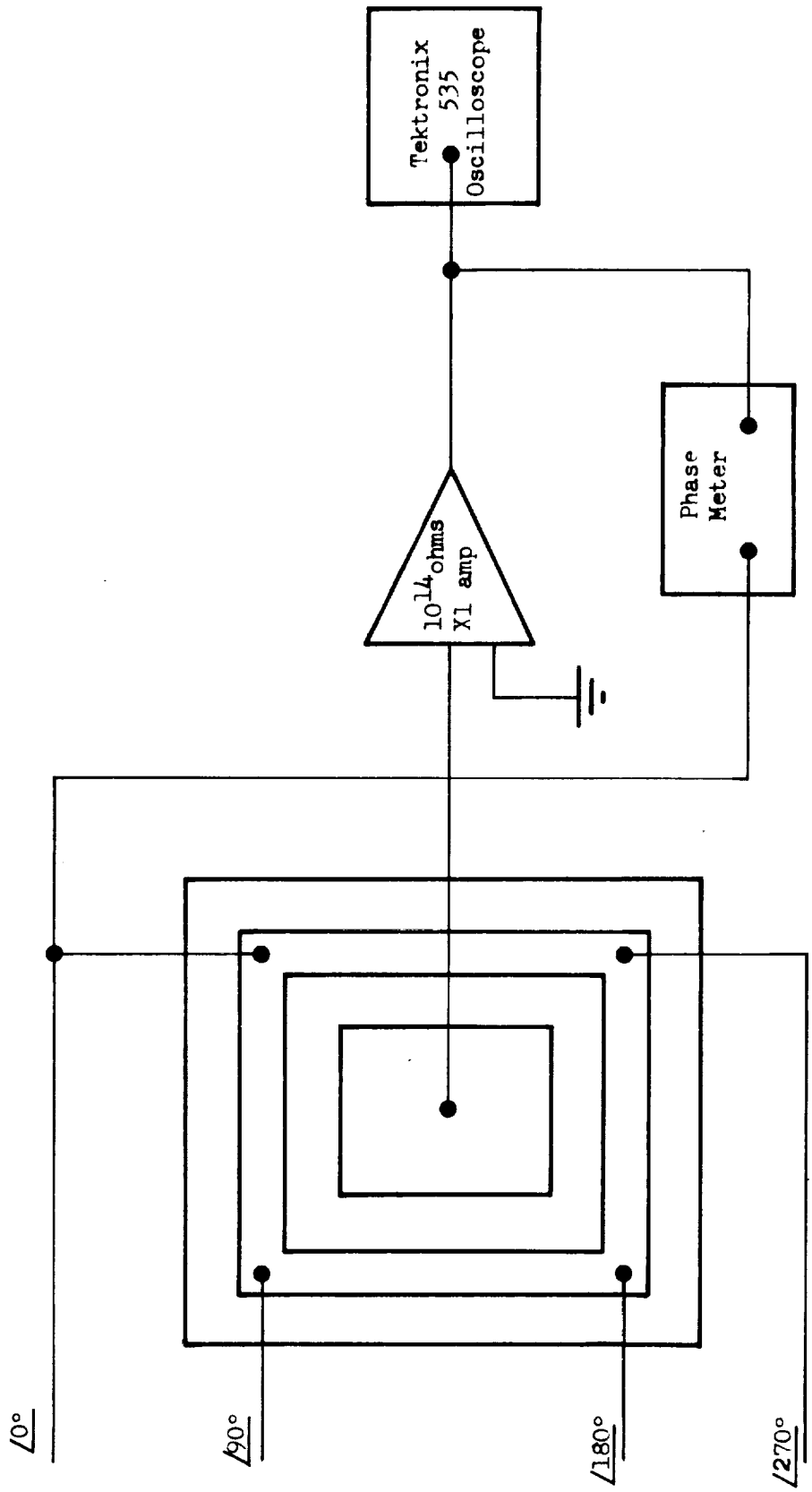

Fig. 25. Readout Circuitry

Figures 26, 27, and 28 show plots of the two-axis position sensitive data. Each device is interrogated with the 1.3 mil diameter light spot with an intensity of approximately a -2.5 m_v star. In each figure there are two numbers printed at each point of interrogation with the light spot. The top number is the phase of the output voltage and the bottom number is the peak-to-peak amplitude in mv. From these data, constant-phase lines and equipotential lines were drawn by interpolation between the measured values.

Detectors 1-25-3C and 1-25-3D were the two devices which were least sensitive to a star image during the uniformity testing. To compensate for this lack of sensitivity, these two detectors were driven at a higher level of 2 v peak-to-peak. The constant-phase and equipotential lines in these detectors are extremely distorted and unusable for any position information.

The data shown in Fig. 28 from detector 2-1-1C are only slightly distorted, with a peak error of 10 mil. This detector was driven at each corner with 1 v peak-to-peak, and differed from the others in that it had a much larger star current output in previous tests. An attempt was made to drive the remaining two devices at 1v, but the signal outputs were so low that no usable information could be gained from them.

F. INFLUENCE OF STAR MAGNITUDE AND OFF-ACTIVE AREA COUPLING

All previous tests were made with a star magnitude of about -2.5 m_v. It was desirable to determine if the volume-effect detector would sense a +2.5 m_v star, and to discover the effects of the variation in star intensity on the output voltage. One other point of interest was the effect on the output of a star image just outside the active area. The latter point is significant in a mosaic of small position sensitive detectors in that it is a measure of coupling effects between adjacent active areas.

Detector 1-23-2A was evaluated. The star image was calibrated at intensities equivalent to star magnitudes of -5, -2.5, 0 and +2.5. The star image was positioned off the active area, and the output voltage was monitored as the star was moved towards and onto the active area in 1 mil increments. The data are shown in Fig. 29. The line through the center of the figure represents the point where the star image first makes contact with the active area. Each unit across the bottom represents a 1 mil motion. Minus values of displacement indicate that the image is off the active area. In this region, the spot is still on the CdS film since the CdS extends about 10 mil beyond the top electrode. The plus values of displacement indicate that the spot is on the active area.

As can be seen from the figure, there is a definite effect on the output as the star intensity is changed. This effect is particularly large for the dimmer stars. Also seen from the figure is that as the star intensity increases, the influence of the star off the active area increases. The largest effect is from the -5 m_v star, which begins to be seen when it is 4.5 mil from the edge. Much of this effect is probably due to light scattering at the substrate.

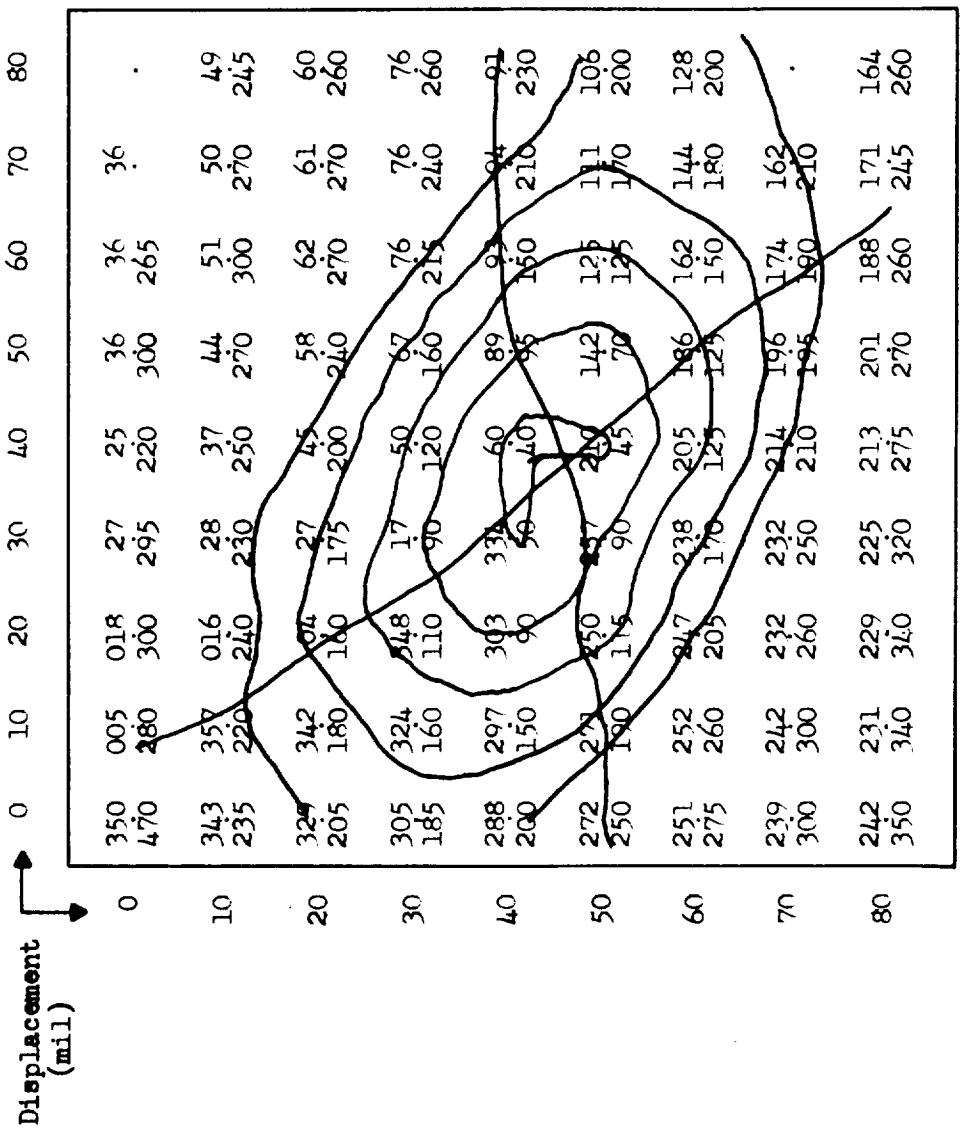

Fig. 26. Two-Axis Position Data, Detector 1-25-3C

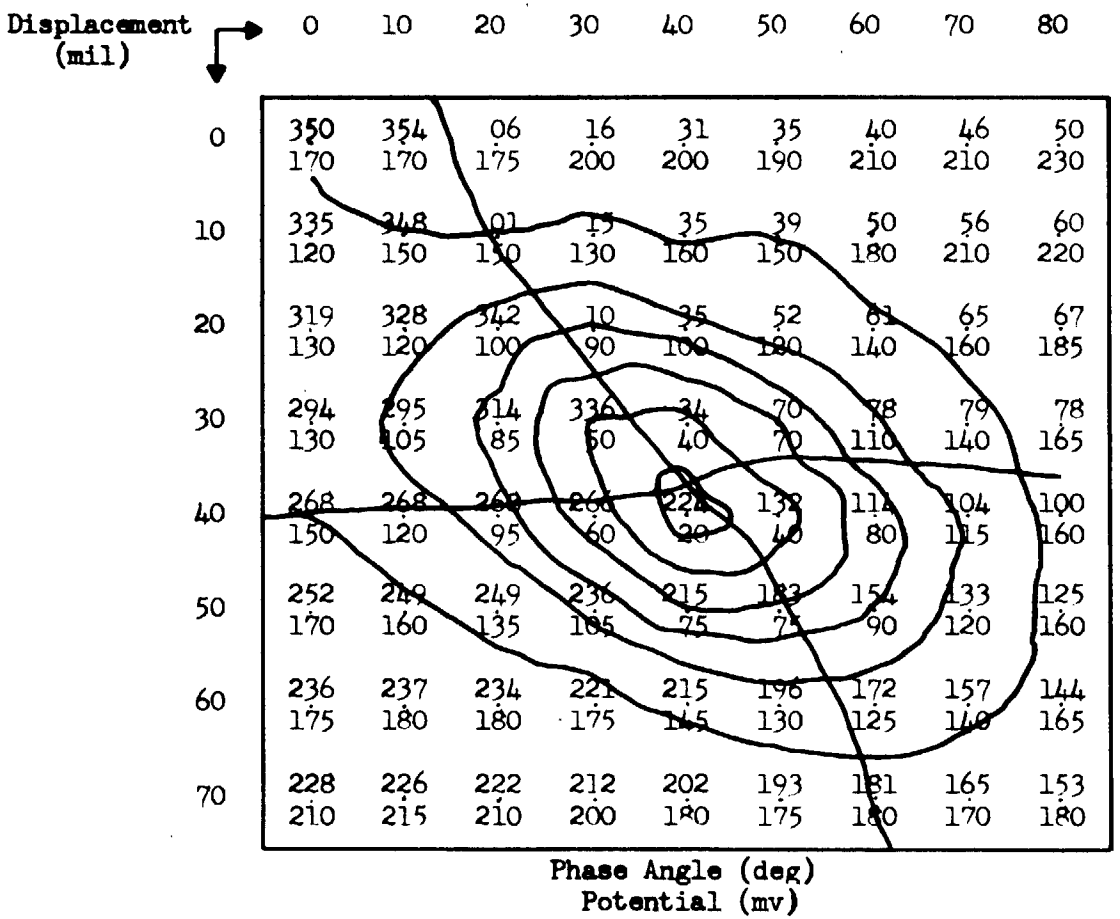

Fig. 27. Two-Axis Position Data, Detector 1-25-3D

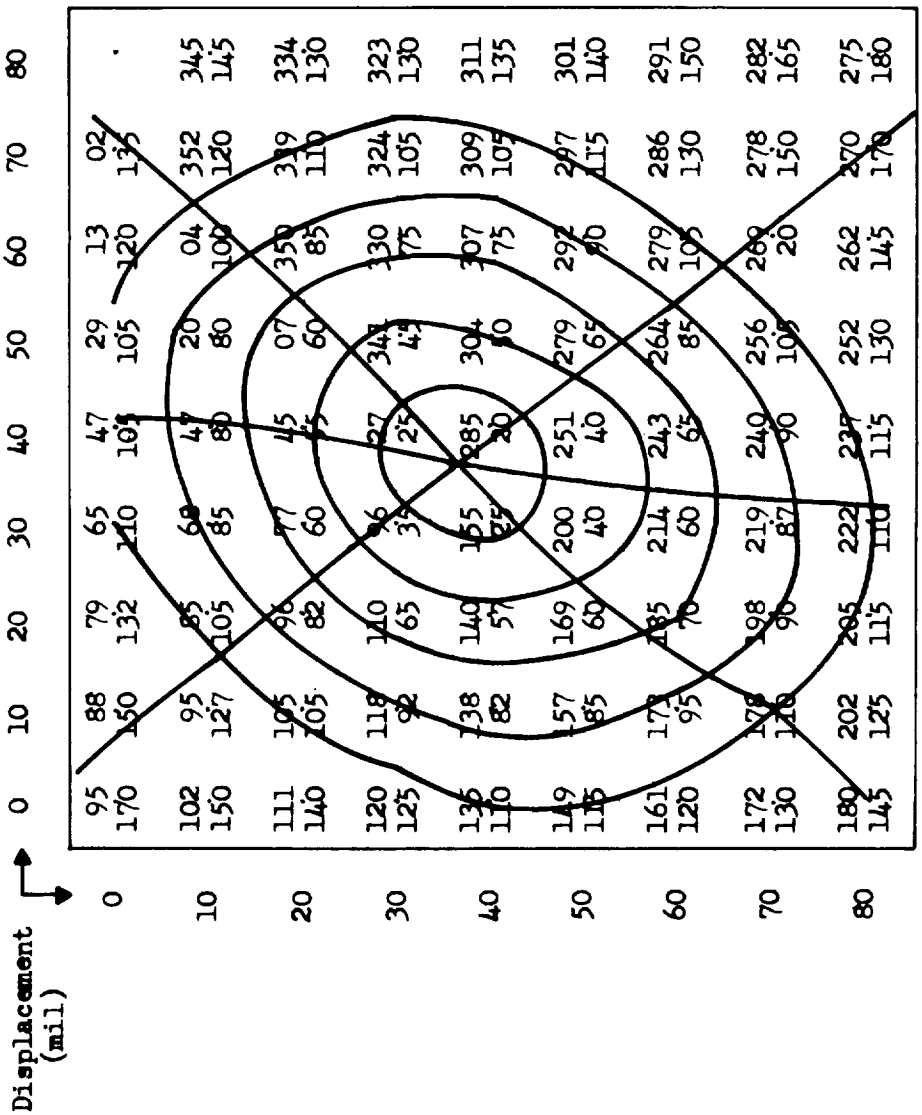

Fig. 28. Two-Axis Position Data, Detector 2-1-1C

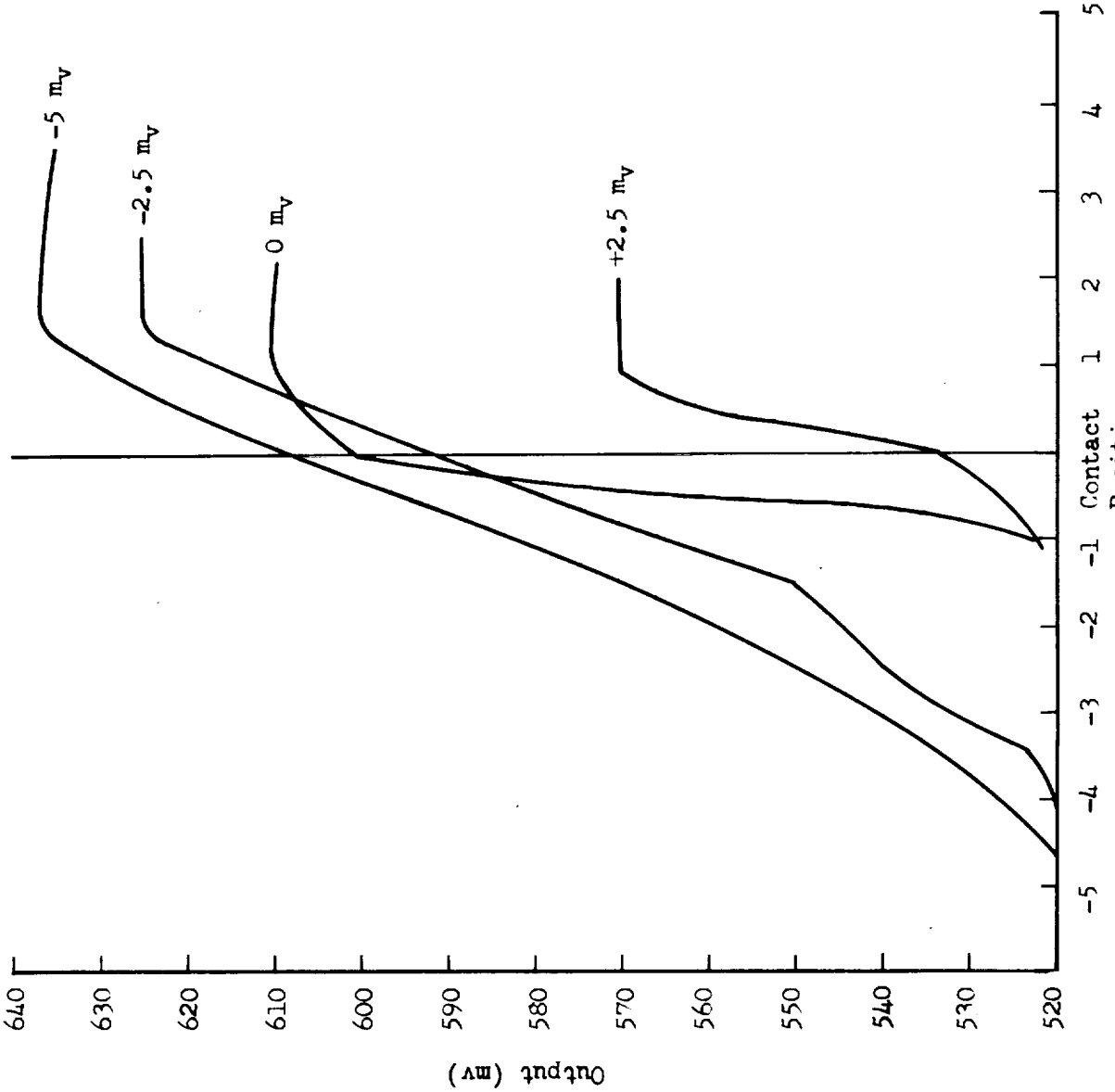

Fig. 29. Off-Active Area Star Influence

VIII. CONCLUSIONS

There are many conclusions which can be drawn from the results of this program. Some of these are of a general nature and others are very specific and relate to a particular detector configuration.

The first and most fundamental of all the information gained is that the general concept of generating an electric field in a tin oxide film and impressing the potential at a point through a CdS film onto an upper electrode is sound. In the past, similar devices which have been made for this application have made use of a current output from the device. The current output is determined by the amount of resistive material such as tin oxide through which current must pass. To Autonetics knowledge, this is the first time a direct voltage output has been achieved. The advantage of the voltage output technique is that complex field patterns can be generated under the CdS and not be perturbed by current flow into the output circuit. As has been shown experimentally, this technique has another advantage in that nonuniformities in photocurrents over the area of a device are not directly reflected as an output error. This is done by having the output circuit impedance high compared to the photoconductive film. The high output circuit impedance causes variations in the resistance of the photoconductor (when a star image is present) to be negligible.

Five detectors were evaluated in this study. All five were tested in the single-axis dc mode, two in the two-axis separate-electrode configuration, and three in the two-axis continuous-electrode configuration.

Evaluation of the data from these tests indicates that at this point in development, the single-axis dc mode is the most accurate. The addition of two more separated electrodes to make the single-axis dc device a two-axis device will always cause a perturbation in the original electric field. One of the objectives of this study was to determine the extent ot this perturbation factor. Comparison of the best data from each shows that the peak position error is more than doubled with the addition of the other electrodes.

The best data from the ac rotating field detectors showed a peak error of 10 percent (0.010 in. error in a 0.100 in. device). Since this is the first known data of this nature, it is felt that the errors can be substantially reduced in the future. The main difference in the three detectors tested in the continuous electrode configuration is that the two devices in which the output field patterns were extremely distorted were the two which were the least sensitive to the star image. It appears that, with a sufficiently large ratio of star current to dark current, the major cause of inaccuracy is in the field produced in the tin oxide itself. It is believed that improvements in detector accuracy will come through improvements in this field pattern. In the devices which were fabricated for these tests it is not definitely known that the field in the tin oxide was any better than the data achieved from the best device. Further work in this area would definitely include the development of more sophisticated techniques to arrive at the best possible field pattern under the CdS film.

The size of the detector active area (90 x 90 mil) is commensurate with an application where the detectors are arranged in a mosaic of from 5 to 10 per inch. The detector performance and ease of fabrication are increased as size decreases to a reasonable limit, since pinhole problems are reduced.

It is felt that the main contribution of this study has been the determination of the following facts about position sensitive volume effect detectors:

(1) The basic concept of potential pickoff via a star image has been proved to be sound.

(2) A technique has been found in which simultaneous two-axis position information can be determined. The first test using this technique resulted in a peak error of 10 percent.

(3) Single-axis position sensitive detectors were evaluated in which the best detector had a peak error of 4 percent.

(4) It was determined that nonuniformities in the detector photocurrent do not couple directly with position error if a voltage output mode of operation is used.

(5) If a photoconductor of sufficient quality is used, the major contributing factor to position error is the generation of the required field pattern.

(6) The area of materials development which is required for practical position sensitive detectors has been determined.

Of all of the significant aspects described above, the latter is the most significant in terms of "where do we go now". Prior to the beginning of the testing it was thought that all five devices were of a sufficient quality that position data would be meaningful. The study resulted in a much more accurate determination of what is really required of the photoconductive material.

Future work along these lines must start with material improvements so that the photoconductor consistently has a large ratio of star current to dark current, without as much preoccupation with photocurrent uniformity. Materials for the transparent electrodes and external electrodes must be optimized. Material improvements must necessarily come through determination and alleviation of the problems of interactions among the detector materials by the establishment of a compatible sequence of fabrication processes. Improvements in the technique for generation of an electric field must be pursued as well as the investigation of new techniques and different types of field patterns. The time and temperature stability of these detectors has not yet been investigated and should be evaluated in future studies. The combination of these developments will make the position sensitive volume effect detector a practical device.

REFERENCES

1. Rose, A., Concepts in Photoconductivity and Allied Problems, Interscience, N.Y. London, 1963

2. Bube, R. H., Photoconductivity of Solids, Wiley, N.Y. London, 1962

3. Moss, T. S., Photoconductivity in the Elements, Academic, New York, 1952

4. Böerr, Esbitt and Kaufman, J. A. P., Volume 37, 7, page 2664